Trisubstituted Heteropolytungstates as Soluble Metal Oxide Analogues. 3.[1] Synthesis, Characterization, ^{31}P, ^{29}Si, ^{51}V, and 1- and 2-D ^{183}W NMR, Deprotonation, and H^+ Mobility Studies of Organic Solvent Soluble Forms of $H_xSiW_9V_3O_{40}^{x-7}$ and $H_xP_2W_{15}V_3O_{62}^{x-9}$

Richard G. Finke,*[2a] Brian Rapko,[2a] Robert J. Saxton,[2a] and Peter J. Domaille[2b]

Contribution from the Department of Chemistry, University of Oregon, Eugene, Oregon 97403, and Central Research and Development Department, E. I. du Pont de Nemours and Co., Experimental Station, Wilmington, Delaware 19898. *Received August 19, 1985*

Abstract: The trivanadium(V)-substituted polyoxoanions A-β-$H_xSiW_9V_3O_{40}^{x-7}$ and $H_xP_2W_{15}V_3O_{62}^{x-9}$ have been synthesized from their lacunary precursors A-β-$SiW_9O_{34}^{10-}$ and $P_2W_{15}O_{56}^{12-}$ and fully characterized. Specifically, $K_6HSiW_9V_3O_{40}\cdot 3H_2O$, $(Bu_4N)_4H_3SiW_9V_3O_{40}$, $(Bu_4N)_{7-x}H_xSiW_9V_3O_{40}$ (x = 0-2), $K_8HP_2W_{15}V_3O_{62}\cdot 9H_2O$, $(Me_4N)_6H_3P_2W_{15}V_3O_{62}\cdot 6H_2O$, $(Bu_4N)_5H_4P_2W_{15}V_3O_{62}$, $(Bu_4N)_6H_3P_2W_{15}V_3O_{62}$, $(Bu_4N)_3KH_5P_2W_{15}V_3O_{62}\cdot 5DMF$, and $(Bu_4N)_{9-x}H_xP_2W_{15}V_3O_{62}$ (x = 0-2) have been prepared and characterized by elemental analysis, thermal gravimetric analysis, solution molecular weight measurements or FAB mass spectroscopy (for $K_6HSiW_9V_3O_{40}\cdot 3H_2O$), IR, and ^1H, ^{29}Si, ^{31}P, ^{51}V, ^{183}W, $^{183}W\{^{51}V\}$, and 2-D $^{183}W\{^{51}V\}$ NMR. The results unambiguously demonstrate the A-β structure of the previously unknown A-β-$SiW_9V_3O_{40}^{7-}$, the adjacent edge-sharing octahedral, or "cap" positions of the three vanadiums in $P_2W_{15}V_3O_{62}^{9-}$, and they provide the first Bu_4N^+ salt, organic solvent soluble forms of $H_xSiW_9V_3O_{40}^{x-7}$ and $H_xP_2W_{15}O_{62}^{x-9}$. The stepwise deprotonation of $(Bu_4N)_4H_3SiW_9V_3O_{40}$ and $(Bu_4N)_5H_4P_2W_{15}V_3O_{62}$ by $Bu_4N^+OH^-$ in CH_3CN has been studied in detail including documentation of the previously unexplained effects of the degree of protonation, dry vs. wet solvents, and added bases or acids upon ^{29}Si, ^{31}P, ^{51}V, and ^{183}W NMR. The studies on $(Bu_4N)_6HSiW_9V_3O_{40}$ proved especially informative, unequivocally establishing its C_s symmetry, A-β-$HSiW_9V_3O_{40}^{6-}$ structure by ^{51}V, ^{183}W, $^{183}W\{^{51}V\}$, and 2-D $^{183}W\{^{51}V\}$ NMR and establishing the H_2O, pyridine (py), and $pyH^+CF_3CO_2^-$ assisted H^+ mobility in $HSiW_9V_3O_{40}^{6-}$. These results allow $HSiW_9V_3O_{40}^{6-}$ to serve as a homogeneous model for H^+ mobility on a heterogeneous oxide surface and, when combined with literature studies of reduced heteropolyanions ("heteropoly blues"), a homogeneous model for H· ($H^+ + e^-$) spillover. The finding of a four-bond vanadium to tungsten ($^4J_{V\text{-}O\text{-}W}$) coupling, the problems in the synthesis and characterization of organic solvent soluble R_4N^+ salts of polyoxoanions, and the significance, implications, and future directions of this work are also presented and discussed.

Polyoxoanions[3] consist of a close-packed array of oxide anions and, as such, can be regarded as discrete fragments of extended metal oxide lattices[4] (Figure 1). Since 1979 we have pursued a program aimed at exploiting this property by focusing upon the preparation of a series of C_{3v} symmetry, Bu_4N^+ counterion and, therefore, organic solvent soluble trisubstituted heteropolyanions $SiW_9M_3O_{40}^{y-}$ (Figure 2A) and $P_2W_{15}M_3O_{62}^{z-}$ (Figure 2B) (M = V^{5+}, Nb^{5+}, Ta^{5+}, Ti^{4+}, Zr^{4+}, Hf^{4+}). One of our goals is to compare these polyoxoanions to their parent oxides M_2O_5 (M = V, Nb, Ta) and MO_2 (M = Ti, Zr, Hf).[1a] A second goal is to exploit their anticipated significant surface change density at oxygen for the support of organotransition-metal catalysts or catalyst precursors.[1] Our third, longer term, and major goal is to use the resultant "solubilized heterogeneous catalysts" to probe the fascinating opportunities that exist for new types of catalysts, for needed spectroscopic models of oxide-supported heterogeneous catalysts and chemisorbed species, and for the insights that should result from detailed mechanistic studies of such soluble, oxide-supported catalysts. Vanadium (V^{5+}) containing polyoxoanions with surface-supported transition metals have not been previously described[1b,c] but accrue additional interest due to the role of V^{5+} containing heteropolyanions in Wacker chemistry as $Pd^{0/2+}$ re-oxidation catalysts.[5] Prior to presenting the results of the present study, important previous work deserves mention and it will prove useful to follow this by a list of the problem areas that existed when we began these studies.

Our approach and focus toward A-$SiW_9M_3O_{40}^{y-}$ and $P_2W_{15}M_3O_{62}^{y-}$ trisubstituted with higher valent metals like M^{4+} and M^{5+} builds upon the findings of Tézé, Pope, and co-workers[6a]

(1) (a) Part 1: Finke, R. G.; Droege, M. W. *J. Am. Chem. Soc.* **1984**, *106*, 7274. One conclusion of this paper is that the trisubstituted heteropolytungstate dimer, $Si_2W_{18}Nb_6O_{77}^{8-}$, behaves, in effect, as a solubilized piece of $(Nb_2O_5)_3$ sandwiched between two "$SiW_9O_{31}^{4-n}$ heteropolytungstate fragments. (b) Part 2: Finke, R. G.; Rapko, B. *Organometallics* **1985**, *4*, 175. (c) Part 4: Finke, R. G.; Rapko, B., manuscript in preparation. (d) Formation of the disubstituted dimers[1e] $[PW_9M_2(H_2O)O_{34}]_2^{10-}$ and[1f] $[P_2W_{15}M_2(H_2O)O_{56}]_2^{12-}$ occurs when B-$PW_9O_{34}^{9-}$ and $P_2W_{15}O_{56}^{12-}$ are treated with low-valent metals, M^{n+}, such as Co^{2+} and Zn^{2+}. (e) Finke, R. G.; Droege, M.; Hutchinson, J. R.; Ganzow, O. *J. Am. Chem. Soc.* **1981**, *103*, 1587. (f) Finke, R. G.; Droege, M. W. *Inorg. Chem.* **1983**, *22*, 1006.

(2) (a) Department of Chemistry, University of Oregon, Eugene, OR 97403. (b) Central Research and Development Department, E. I. du Pont de Nemours and Co. Experimental Station, Wilmington, DE 19898. Contribution 3672.

(3) Pope, M. T. In "Heteropoly and Isopoly Oxometallates"; Springer-Verlag: New York, 1983.

(4) This feature was first noted by Baker in 1961. Baker, L. C. W. In "Advances in the Chemistry of Coordination Compounds"; Kirschner, S., Ed.; MacMillan: New York, 1961; p 604.

(5) (a) Kozhevenikov, I. V.; Matveev, K. I. *Appl. Catal.* **1983**, *5*, 135; *Russ. Chem. Rev. (Eng. Transl.)* **1982**, *51*, 1075. (b) Ogawa, H.; Fujinami, H.; Taya, K.; Teratani, S. *J. Chem. Soc., Chem. Commun.* **1981**, 1274. (c) Taraban'ko, V. E.; Kozhevenikov, I. V.; Matveev, K. I. *Kinet. Katal.* **1978**, *19*, 1160. (d) Davidson, S. F.; Mann, B. E.; Maitlis, P. M. *J. Chem. Soc., Dalton Trans.* **1984**, 1223.

(6) (a) Mossoba, M. M.; O'Connor, C. J.; Pope, M. T.; Sinn, E.; Hervé, G.; Tézé, A. *J. Am. Chem. Soc.* **1980**, *102*, 6864. (b) Harmalker, S. P.; Leparulo, M. A.; Pope, M. T. *J. Am. Chem. Soc.* **1983**, *105*, 4286. Harmalker, S. P.; Pope, M. T. *J. Am. Chem. Soc.* **1981**, *103*, 7381. This earlier synthesis is summarized below:

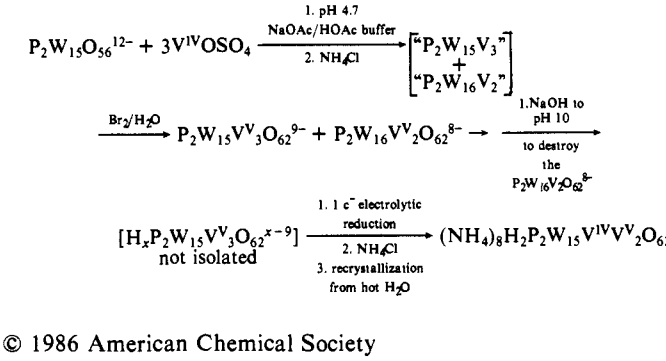

0002-7863/86/1508-2947$01.50/0

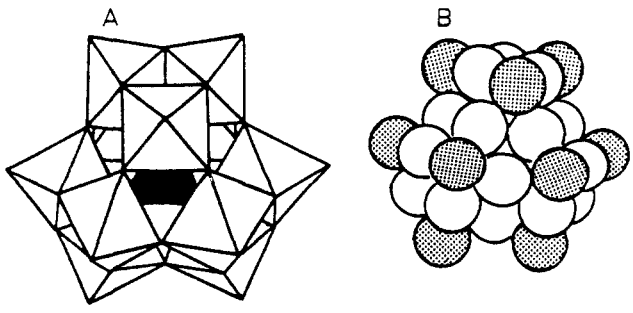

Figure 1. Polyhedral (A) and space filling (B) representations of α-$SiW_{12}O_{40}^{4-}$. In the polyhedral representation, A, the central phosphate is represented as the black tetrahedron. Tungsten atoms are located at the center of each octahedra with oxygens at the vertices. The edge- and corner-shared oxygens of the WO_6 octahedra are easily distinguished in three of the four W_3O_{13} triads of edge-shared octahedra (centered at 12 o'clock, 4 o'clock, and 8 o'clock) that are visible here. The space filling model, B, shows the close-packed arrangements of the oxide anions with the shaded circles representing terminal oxygens.

and those of Harmalker, Leparulo, and Pope[6b] demonstrating that A-α-$SiW_9V_3O_{40}^{7-}$ and $P_2W_{15}V_3O_{62}^{9-}$, respectively, can be prepared. Also relevant is our work showing that B-$PW_9O_{34}^{9-}$ and $P_2W_{15}O_{56}^{12-}$ form disubstituted dimers rather than $PW_9M_3O_{40}^{y-}$ and $P_2W_{15}M_3O_{62}^{z-}$ when lower M^{2+} such as Co^{2+} and Zn^{2+} are used.[1d-f] In spite of this previous work, a significant number of problems remained at the onset of the present studies,[7] even for the V^{5+} derivatives A-β-$H_xSiW_9V_3O_{40}^{x-7}$ and $H_xP_2W_{15}V_3O_{62}^{x-9}$. Only a one-line sentence in a footnote[6a] has been published for A-α-$SiW_9V_3O_{40}^{7-}$ and A-β-$SiW_9V_3O_{40}^{7-}$ has not been previously described. The previous synthesis of $P_2W_{15}V_3O_{62}^{9-}$ was the result of work focused toward the V^{IV} derivative ($P_2W_{15}V_2V^{IV}O_{62}^{10-}$) for ESR studies, so that the reported synthesis of $P_2W_{15}V_3O_{62}^{9-}$ is without isolation in an unknown yield and required unnecessary steps.[6b] In our work, the proper choice of pH, countercation, the variable number x of H^+ for different countercations, and the solvents for the synthesis and recrystallization of $H_xSiW_9V_3O_{40}^{x-7}$ and $H_xP_2W_{15}V_3O_{62}^{x-9}$ and their characterization—especially as their previously unknown R_4N^+ salts—has required a significant amount of effort and extensive ^{31}P, ^{29}Si, ^{51}V, and ^{183}W NMR time. In the synthesis of $(Bu_4N)_6H_3P_2W_{15}V_3O_{62}$, for example, "simple" metathesis from K^+ to $(Bu_4N)^+$ yielded a $(Bu_4N)_{9-x}H_xP_2W_{15}V_3O_{62}$ product of *varying* Bu_4N^+ even when the solution pH was carefully controlled. The above illustrates some of the problems and pitfalls that were not well documented in the polyoxoanion area[7] which

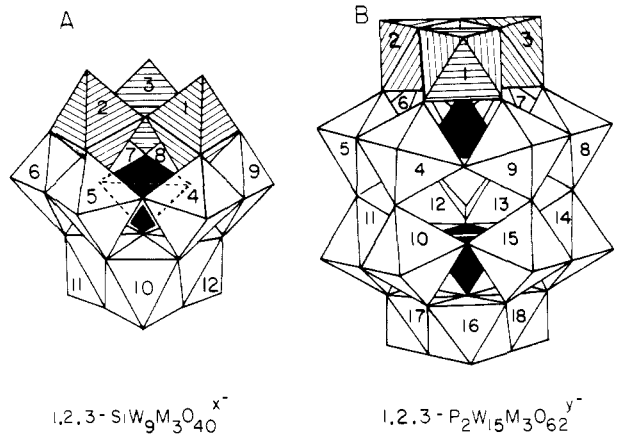

Figure 2. Polyhedral representations of (A) α-(1,2,3) $SiW_9M_3O_{40}$ (A-type derivative) and (B) α-(1,2,3) $P_2W_{15}M_3O_{62}$ (B-type derivative). The octahedra with hatched lines represent those of the substituted metal vanadium. The A isomer refers to the presence of a triad of corner-sharing (W_1, W_2, W_3 in 2A) octahedra and the B isomer refers to the presence of a triad of edge sharing (W_1, W_2, W_3 in 2B) octahedra (see also Figure 6). The M–O–M angle in an A isomer is about 150°, as compared to the about 125° M–O–M angle in the B isomer. The α isomerism refers to the arrangement of the W_{10}, W_{11}, W_{12} triad in (A) or the W_{16}, W_{17}, W_{18} triad in (B), each of which would be rotated by $\pi/3$ in a β isomer (see also Figure 10).

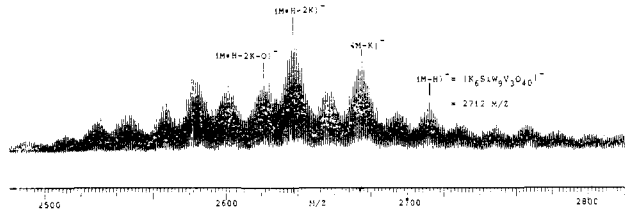

Figure 3. FAB negative ion mass spectrum of $K_6HSiW_9V_3O_{40}$ dissolved in a thioglycerol matrix. A $[MH]^-$ = $[K_6SiW_9V_3O_{40}]^-$ parent ion at m/z = 2712 is observed along with extensive K^+ for H^+ exchange (cationization), peaks due to the loss of O (m/z = 16), and peaks due to the loss of WO_3 (m/z = not shown). The envelopes of higher molecular weight (above 2712) are separated by m/z 18, suggesting that they are $(H_2O)_n$ adducts.

are addressed by the present studies. Additionally, it was not clear at the beginning of our work whether or not the deprotonation of $H_xSiW_9V_3O_{40}^{x-7}$ or $H_xP_2W_{15}V_3O_{62}^{x-9}$ could be achieved without decomposition, since $SiW_{12}O_{40}^{4-} + OH^-$ rapidly degrades to SiO_3^{2-} and WO_4^{2-} ($t_{1/2}$ in the range of seconds to minutes depending upon the exact conditions)[8] and since $P_2W_{16}V_2O_{62}^{8-}$ is known to be degraded by base.[6b] Finally, the multiple line and/or broadened ^{51}V and ^{183}W NMR of protonated R_4N^+ salts of polyoxoanions in dry organic solvents was not previously documented and was a significant impediment to our early studies.

Herein we report the full details of our synthesis and characterization by elemental analysis, TGA, solution molecular weight measurements, FAB/mass spectroscopy (FABMS),[9] IR, and ^{31}P, ^{29}Si, ^{51}V, and ^{183}W NMR of $K_6HSiW_9V_3O_{40}$ and $(Bu_4N)_4H_3SiW_9V_3O_{40}$. The stepwise deprotonation and H^+ mobility studies starting with $(Bu_4N)_4H_3SiW_9V_3O_{40}$ are reported with an emphasis upon monoprotonated $(Bu_4N)_6HSiW_9V_3O_{40}$, including its detailed structure as elucidated by 1- and 2-D ^{183}W and $^{183}W\{^{51}V\}$ NMR. Simplified, high-yield syntheses for (cation)$_{9-x}H_xP_2W_{15}V_3O_{62}$ (cation = K^+ (x = 8), Me_4N^+ (x = 6),

(7) (a) Some previously documented problems in the synthesis and characterization of polyoxoanions include difficulties in obtaining reliable elemental analyses,[7b] in obtaining X-ray diffraction structures,[7c] and in obtaining accurate solution molecular weights.[7d] Some additional problems, many of which were uncovered by the present studies, are problems in the NMR of protonated anions in *dry* organic solvents,[7e] in the (non)crystallization of Keggin (e.g., $SiW_9V_3O_{40}^{7-}$) and Dawson (e.g., $P_2W_{15}V_3O_{62}^{9-}$) anions containing greater than four and six Bu_4N^+ counterions, respectively,[7e,f] and in the thermal isomerism of some polyoxoanions.[7g] An additional difficulty stems from the absence, to date, of chromatographic methods (except in rare[6b] instances), leaving only recrystallization as the purification method and requiring ^{31}P, ^{29}Si, or ^{51}V or other *sensitive* NMR methods, rather than chromatographic methods, as the criterion of homogenity. (b) See the results and discussion in: Finke, R. G.; Droege, M. W. *Inorg. Chem.* **1983**, *22*, 1006. Smith, D. P.; Pope, M. T. *Anal. Chem.* **1969**, *40*, 1906. Fernandez, M. A.; Bastiaans, G. J. *Anal. Chem.* **1979**, *51*, 1402. A reliable determination of the number of oxygen atoms is a major step toward avoiding misformulated polyoxoanions. For $K_6HSiW_9V_3O_{40}$ (see the text) and elsewhere[9b] we have shown how elemental analysis combined with FABMS can fulfill this need in favorable cases. See also ref 32. (c) Evans, H. T., Jr.; Pope, M. T. *Inorg. Chem.* **1984**, *23*, 501. Acerete, R.; Hammer, C. F.; Baker, L. C. W. *Inorg. Chem.* **1984**, *23*, 1478 and references therein. (d) See the supplemental materials for ref 1a and the discussion and references therein. (e) See the results presented in the text. (f) For example, $ZnW_{12}O_{40}^{6-}$ and $AlW_{12}O_{40}^{5-}$ are obtained as crystalline salts with only four Bu_4N^+ cations: Nomiya, K.; Miwa, M. *Polyhedron* **1983**, *2*, 955. We find that $(Bu_4N)_4H_3SiW_9V_3O_{40}$, $(Bu_4N)_4[CpTi{\cdot}SiW_9V_3O_{40}]$, and $(Bu_4N)_6H_3P_2W_{15}V_3O_{62}$ are crystalline while $(Bu_4N)_7SiW_9V_3O_{40}$, $(Bu_4N)_7SiW_9Nb_3O_{40}$,[1a] $(Bu_4N)_5[(C_5Me_5)Rh{\cdot}SiW_9Nb_3O_{40}]$,[1a] $(Bu_4N)_9P_2W_{15}V_3O_{62}$, and $(Bu_4N)_9P_2W_{15}Nb_3O_{62}$ are not, in our hands. Crystallization attempts with other, smaller cations should solve this problem and are in progress. (g) See ref 1e,f and 37.

(8) (a) Kepert, D. L.; Kyle, J. H. *J. Chem. Soc., Dalton Trans.* **1978**, 137; (b) *J. Chem. Soc., Dalton Trans.* **1978**, 1781. (c) These papers[8a,b] report a significant polyoxoanion stabilization effect toward OH^- degradation by R_4N^+ counterions.

(9) (a) Finke, R. G.; Droege, M. W.; Cook, J. C.; Suslick, K. S. *J. Am. Chem. Soc.* **1984**, *106*, 5750. The K^+ salt referred to as "$K_4H_3SiW_9V_3O_{40}$" therein is correctly reformulated as $K_6HSiW_9V_3O_{40}$ based on a K^+ analysis (Experimental Section). (b) Suslick, K. S.; Cook, J. C.; Rapko, B.; Droege, M. W.; Finke, R. G. *Inorg. Chem.* **1986**, *25*, 241.

Bu_4N^+ (x = 5)), their characterization, and deprotonation studies of $(Bu_4N)_5H_4P_2W_{15}V_3O_{62}$ are also reported.

Results and Discussion

(I) Synthesis of A-β-$K_6HSiW_9V_3O_{40}$ and A-β-$(Bu_4N)_4H_3SiW_9V_3O_{40}$. The trisubstituted heteropolytungstate $H_xSiW_9V_3O_{40}^{x-7}$ can be obtained as the K^+ or Bu_4N^+ salt from the reaction of solid A-β-$Na_9HSiW_9O_{34}\cdot 23H_2O$[10] added to a vigorously stirred solution of sodium metavanadate at pH ≃1.5, where VO_2^+ forms in aqueous solution,[11] according to the following stoichiometry:

$$HSiW_9O_{34}^{9-} + 3VO_3^- + (5 + x)H^+ \rightarrow H_xSiW_9V_3O_{40}^{x-7} + 3H_2O \quad (1)$$

Following the facile initial synthesis of the $H_xSiW_9V_3O_{40}^{x-7}$ anion (indicated by the rapid development of a deep cherry-red solution upon addition of the lacunary heteropolytungstate to the pale yellow vanadate solution), conversion to the potassium salt allows isolation of the trisubstituted heteropolyanion in a form that can be purified rapidly and in good yield (82% from $SiW_9O_{34}^{10-}$ on a 37-g scale by recrystallization from hot aqueous solutions and drying at 25 °C under vacuum). Evidence for the composition $K_6HSiW_9V_3O_{40}\cdot 3H_2O$ is provided by the elemental analysis for K^+, by thermal gravimetric analysis (TGA) (calcd for $3H_2O$ 2.0%; found 1.7%), and especially by FABMS. Previously we presented a preliminary report of the FABMS of $K_6HSiW_9V_3O_{40}$ as part of the first mass spectra reported for polyoxoanions.[9a] Figure 3 presents the negative ion FABMS of $K_6HSiW_9V_3O_{40}$ obtained in thioglycerol. Negative ions for $K_6HSiW_9V_3O_{40}^-$ and $K_5HSiW_9V_3O_{40}^-$ are observed along with extensive exchange of K^+ and H^+ cations (cationization). Loss of O (m/z = 16) and WO_3 (m/z = 232) are other dominant features of both this and other[9a,b] heteropolytungstate FABMS. Significantly, the FABMS firmly and unequivocally establishes the $SiW_9V_3O_{40}^{7-}$ composition of the trisubstituted Keggin anion *including the number of oxygens*, a previously unattainable result even by an expensive and relatively slow Si, W, V, and O elemental analysis.[7a,b] With the molecular composition in hand, the overall C_{3v} symmetry of the $SiW_9V_3O_{40}^{7-}$ anion was readily established by the two-line ^{183}W NMR observed in D_2O, δ −110.4 (6 W), −112.9 (3 W).

Metathesis of the K^+ salt with $Bu_4N^+Br^-$ in acidic, aqueous solution followed by crystallization of the product from acetonitrile/dichloromethane yields the desired $(Bu_4N)_4H_3SiW_9V_3O_{40}$ on a 30–36-g scale (58–70% yield). The success of the K^+/Bu_4N^+ metathesis is critically dependent upon maintaining the solution pH at its initial low, pH ≃1.5 value. Metathesis followed by product precipitation results in an increase in pH and, at pH ≃7, for example, the more soluble, noncrystalline[7f] $(Bu_4N)_6HSiW_9V_3O_{40}$ is formed in low yield.

(II) Characterization of $(Bu_4N)_4H_3SiW_9V_3O_{40}$. (A) Molecular Formula. The molecular formula $(Bu_4N)_4H_3SiW_9V_3O_{40}$ has been determined by elemental analysis, TGA, and solution molecular weight measurements. The elemental analysis for C, H, N, Si, W, V, and O (and Na^+, K^+ = 0) establishes the empirical formula as $[(Bu_4N)_4SiW_9V_3O_{40\pm 2}]_n$ and accounts for 98.8% of the total mass. Thermal gravimetric analysis (TGA) shows no detectable (<0.5%) weight loss below 200 °C indicative of the absence (<1H_2O) of any lattice water[12] in samples dried at 80 °C under vacuum. A solution ultracentrifugation molecular weight measurement[13] was used to confirm that a monomer exists in solution

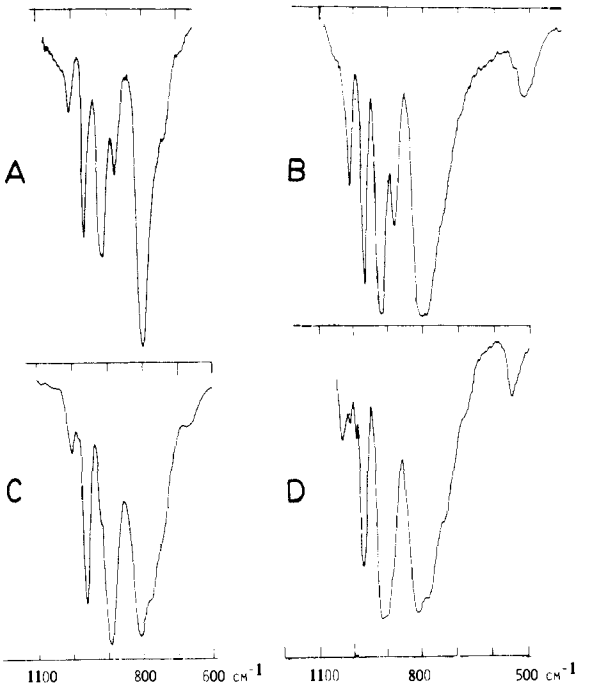

Figure 4. IR spectra of α-$(Bu_4N)_4SiW_{12}O_{40}$ (top, A and B) and A-β-$(Bu_4N)_4H_3SiW_9V_3O_{40}$ (bottom, C and D), taken as CH_3CN solutions (left-hand sides, A and C) and as KBr disks (right-hand side, B and D). Assignments are based by analogy to the literature assignments[12d] of $XW_{12}O_{40}^{n-}$ and are indicated in the text.

[calcd for $(Bu_4N)_2H_3SiW_9V_3O_{40}^{2-}$,[7a,d] 2963; found, 3076 (Figure 1a, supplemental materials)], but the most compelling evidence for the $SiW_9V_3O_{40}^{7-}$ formulation is the FABMS of the potassium salt. The seven minus charge on the $SiW_9V_3O_{40}^{7-}$ anion and the presence of only four Bu_4N^+ but no Na^+ or K^+ by analysis and no H_2O (or H_3O^+) by TGA require the presence of three H^+ for charge balance, $(Bu_4N)_4H_3SiW_9V_3O_{40}$. The presence of three H^+ is also fully supported by a pH titration and pH vs. ^{51}V and ^{183}W NMR titrations detailed in section III. Several attempts to directly observe these protons by ^1H NMR in dry Me_2SO-d_6 or dry CD_3CN failed, however, with only the expected resonances for Bu_4N^+ being observed.

(B) IR Spectroscopy. In the absence of ^{31}P, ^{29}Si, ^{51}V, and ^{183}W NMR, the IR of polyoxoanions is useful for comparison to the IR of authentic samples (as well as the assignment of α,β isomers),[14] so that the IR of $(Bu_4N)_4H_3SiW_9V_3O_{40}$ in CH_3CN and as KBr disks in comparison to that of $(Bu_4N)_4SiW_{12}O_{40}$ has been included in Figure 4. By analogy to the assignments for other $XM_{12}O_{40}^{n-}$ Keggin anions,[12d] the ~960-cm^{-1} band, the broader ~900-cm^{-1} band, and the very broad ~800-cm^{-1} band can be assigned to W=O, Si—O and overlapping corner-sharing octahedra M—O—M, and edge-sharing octahedra M—O—M vibrations, respectively. These assignments have proven of value in establishing the site of $CpTi^{3+}$ attachment to $SiW_9V_3O_{40}^{7-}$ since the $CpTi^{3+}$ will perturb and split mainly the M—O—M vibration due to edge-sharing octahedra.[1b,c]

IR spectroscopy also provides evidence that the three protons in $(Bu_4N)_4H_3SiW_9V_3O_{40}$ are present as H^+ as indicated and not as $(H_3O)^+$, a question not resolved by elemental analysis and set at a limit of <1H_3O^+ (i.e., <1H_2O) by TGA. Zeolitic water in heteropolyanions results in a free H_2O bending vibration around 1640 cm^{-1} while H_3O^+ shows a characteristic vibration around 1715 cm^{-1}.[12a] Examination of the IR spectrum of the $(Bu_4N)_4H_3SiW_9V_3O_{40}$ shows no IR bands in the 1800–1600-cm^{-1} region. Control experiments involving stoichiometric addition of water (for the 1640-cm^{-1} band) as well as examination of vacuum dried $(H_3O)_4SiW_{12}O_{40}\cdot XH_2O$ (for the 1715-cm^{-1} band) indicate

(10) (a) Hervé, G.; Tézé, A. *Inorg. Chem.* **1977**, *16*, 2115. (b) Robert, F.; Tézé, A. *Acta Crystallogr., Sect B* **1981**, *B37*, 318.

(11) See the diagram, Figure 3.1, on p 35 in ref 3. By ^{51}V NMR we have shown that at pH 1.5 the $H_3V_{10}O_{28}^{3-} \rightarrow VO_2^+$ conversion is slow at room temperature but is accelerated at pH = 0.7–0.8.

(12) (a) Highfield, J. G.; Moffat, J. B. *J. Catal.* **1984**, *88*, 177. (b) Hodnett, B. K.; Moffat, J. B. *J. Catal.* **1984**, *86*, 253; **1985**, *91*, 93. (c) Tsigdinos, G. A. *Ind. Eng. Chem. Prod. Res. Dev.* **1974**, *13*, 267. (d) Rocchiccioli-Deltcheff, C.; Fournier, M.; Franck, R.; Thouvenot, R. *Inorg. Chem.* **1983**, *22*, 207.

(13) Solution molecular weights for Bu_4N^+ salts of polyoxoanions in CH_3CN are generally high by 10–20%. Possible reasons for this and additional details are presented elsewhere[1a] (see the Supplementary material in 1a).

(14) (a) Thouvenot, R.; Fournier, M.; Franck, R.; Rocchiccioli-Deltcheff, C. *Inorg. Chem.* **1984**, *23*, 598. (b) Reference 12d.

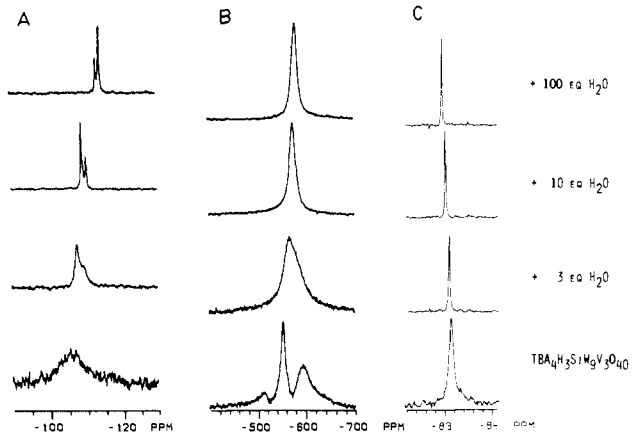

Figure 5. ^{183}W (left, A), ^{51}V (center, B), and ^{29}Si (right, C) NMR spectra as a function of added equivalents of water to an initially dry CD_3CN soluton at 21 °C. Conditions: ^{51}V NMR, 1 g/2 mL of CD_3CN, 12-mm vertical tube, LB = 10, 200 transients, 0.04 min; ^{29}Si NMR, 1 g/3 mL of CD_3CN, 12-mm vertical tube, LB = 1, 7000 transients, 2.5 h; ^{183}W NMR 2 g/3 mL of CD_3CN, 10-mm vertical tube, LB = 1, 10 000 transients, 2.3 h. Due to the insolubility of 2 g of $(Bu_4N)_4H_3SiW_9V_3O_{40}$ in 3 mL of CD_3CN + 100 equiv of water, additional CH_3CN was introduced, bringing the total volume to 4.5 mL to ensure a homogeneous system.

that both H_2O and H_3O^+, if present, should have been observable—suggesting that the proper formulation of this compound is indeed $(Bu_4N)_4H_3SiW_9V_3O_{40}$, with the protons directly attached to the surface of the heteropolytungstate (vide infra).

(C) ^{51}V, ^{29}Si, and ^{183}W NMR Spectroscopic Studies of $(Bu_4N)_4H_3SiW_9V_3O_{40}$. Our two initial goals here were to fully establish the structure of the $SiW_9V_3O_{40}^{7-}$ polyoxoanion and, if possible, to elucidate the surface binding sites of the three attached H^+. Early spectroscopic studies in dry organic solvents such as CD_3CN or Me_2SO-d_6 revealed no obvious resonances in the ^{183}W NMR at reasonable accumulation times and only a puzzling, very broad resonance at ca. −100 ppm following extended acquisition periods for concentrated (>0.1 M) solutions of $(Bu_4N)_4H_3SiW_9V_3O_{40}$. Once a switch to the significantly, ca. 3.6×10^4, more sensitive ^{51}V NMR was made, it became clear that low symmetry and/or multiple forms of the triprotonated $H_3SiW_9V_3O_{40}^{7-}$ (and slow H^+ exchange on the NMR time scale) were present and that addition of H_2O or bases produces an averaged spectrum as documented below.

Figure 5 shows the ^{183}W, ^{51}V, and ^{29}Si NMR of $(Bu_4N)_4H_3SiW_9V_3O_{40}$ in initially dry CD_3CN at 21 °C as a function of added H_2O (0, 3, 10, and 100 equiv of H_2O). The broad, low S/N ^{183}W resonance in Figure 5A is gradually transformed to the expected two lines of 2:1 intensity (six belt W, three cap W; Figure 2A) in the ^{183}W NMR [δ −108.4 (6 W, $\Delta\nu_{1/2}$ = 4.4 ± 0.2 Hz), −110.1 (3 W, $\Delta\nu_{1/2}$ = 4.0 ± 0.4 Hz) with ca. 10 equiv of H_2O]. Concurrently, the three broad ^{51}V lines of approximate relative intensity 1.0, 5.7, and 9.0 collapse to a single, broad ^{51}V resonance (δ −579, $\Delta\nu_{1/2}$ = 1358 ± 4 Hz) with ca. 10 equiv of H_2O. These results require an overall average C_{3v} symmetry for $H_3SiW_9V_3O_{40}^{4-}$ in the presence of H_2O. The ^{29}Si NMR behaves similarly, with the single broadened resonance in dry CD_3CN sharpening to one narrow line at −83.0 ppm ($\Delta\nu_{1/2}$ = 0.52 ± 0.04 Hz) in CD_3CN with ca. 10 equiv of H_2O. The data are consistent with a H_2O-assisted exchange process such as $H_3SiW_9V_3O_{40}^{4-} + H_2O \rightleftharpoons [H_3O^+ + H_2SiW_9V_3O_{40}^{5-}] \rightleftharpoons H_3SiW_9V_3O_{40}^{4-} + H_2O$ that, in the presence of added H_2O, becomes competitive with the ^{51}V and ^{183}W NMR timescales.

It's worth noting that the above results provide a homogeneous model for H^+ mobility on a soluble oxide surface. In heterogeneous catalysis, a similar mechanism for $H^+ + e^-$ ($H\cdot$) migration or spillover has been proposed for H_2-reduced WO_3, i.e., H_2O-assisted H^+ (H_3O^+) mobility on the oxide surface with e^- transfer to W ($W^{VI} + e \rightarrow W^V$) and "$e^-$ mobility" within the oxide[15] (although the mechanism of hydrogen spillover remains controversial).[15e] Moreover, since "e^- mobility" (mixed valence) in heteropolytungstate is well studied,[16] polyoxyanions can now be said to provide a homogeneous model for both the $H^+(H_3O^+)$ and e^- mobility involved in one possible mechanism of H· spillover. The coupling or correlation of the two $H^+ + e^-$ mobilities has not received but deserves study, however.

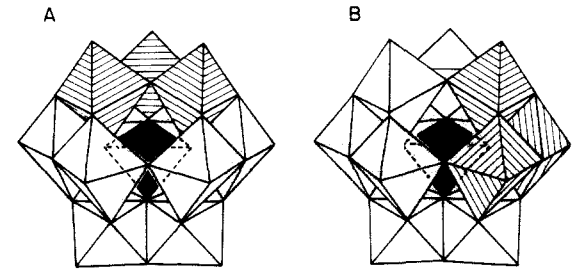

Figure 6. Polyhedral representation of (A) A-β-$SiW_9V_3O_{40}^{7-}$ and (B) B-β-$SiW_9V_3O_{40}$ with the three vanadium represented by the shaded octahedra. Note that the six "belt" W octahedra and the three "cap" W octahedra corner share in the A isomer (A) and edge-share in the B isomer (B). Note further that the B-β isomer obtained by a $\pi/3$ rotation of any triad other than the vanadium-containing triad will result in a lower, C_s, symmetry anion.

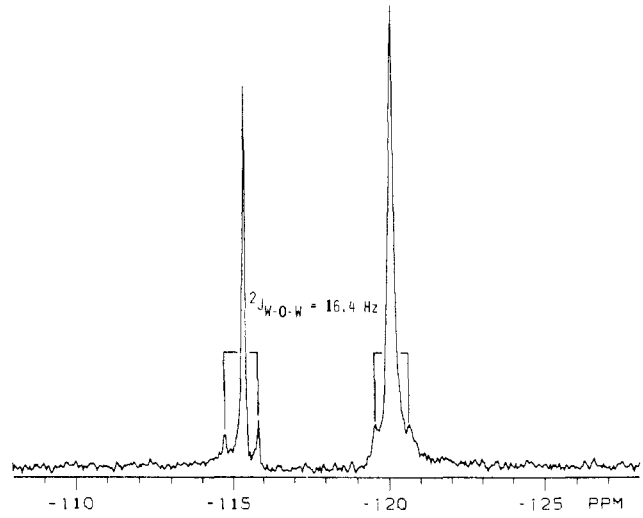

Figure 7. ^{183}W NMR spectrum of the free acid $H_7SiW_9V_3O_{40}$ in D_2O (pD 0.9),[28a] 2 g/mL D_2O, at 21 °C, 10-mm vertical tube, 0.25 LB, 7000 transients, 1.6 h. Central lines are observed at −120.0 (6 W, $\Delta\nu_{1/2}$ = 2.41 Hz, S/N = 78) and ca. 115.4 ppm (3 W, $\Delta\nu_{1/2}$ = 1.32 Hz, S/N = 42) with satellites due to the reciprocal $^2J_{W\text{-}O\text{-}W}$ of 16.4 ± 1.2 Hz being readily apparent.

Returning to the NMR studies of $H_3SiW_9V_3O_{40}^{4-}$, since our synthesis utilized the crystallographically characterized A isomer[10b] of the $SiW_9O_{34}^{10-}$ starting material, we anticipated that the $SiW_9V_3O_{40}^{7-}$ product would retain the A arrangement of a triad of corner-sharing VO_6 octahedra, Figure 6A, rather than the B arrangement of a triad of edge-sharing VO_6 octahedra, Figure 6B. These two possibilities are distinguishable by ^{183}W NMR $^2J_{W\text{-}O\text{-}W}$ couplings since the former, A isomer has a belt of 6 W connected to the 3 W cap via corner-sharing octahedra (Figure

(15) (a) Levy, R. B.; Boudart, M. *J. Catal.* **1974**, *32*, 304. (b) Vannice, M. A.; Boudart, M.; Fripiat, J. J. *J. Catal.* **1970**, *17*, 359. (c) Benson, J. E.; Kohn, H. W.; Boudart, M. *J. Catal.* **1966**, *5*, 307. (d) Pajonk, G. M., Teichner, S. J., Germain, J. E., Eds., "Spillover of Adsorbed Species"; Elsevier: New York, 1983. (e) Dmitriev, R. V.; Steinberg, K.-H.; Detjuk, A. N.; Hofmann, F.; Bremer, H.; Minachev, Kh. M. *J. Catal.* **1980**, *65*, 105 and references therein.

(16) The mixed-valence ("e^- mobility") properties of "heteropoly blues" have received considerable attention. A few leading references include: (a) Pope, M. T. In "Mixed Valence Compounds"; Brown, D. B., Ed.; Reidel Publishing: Dordrecht, Holland, 1980; p 365. (b) Reference 3, p 101–118. (c) Sanchez, C.; Livage, J.; Launay, J. P.; Fournier, M.; Jeannin, Y. *J. Am. Chem. Soc.* **1982**, *104*, 3194. (d) Ciabrini, J. P.; Contant, R.; Fruchart, J. M. *Polyhedron* **1983**, *2*, 1229.

6a) which exhibit larger $^2J_{W-O-W} \sim 13-30$ Hz couplings,[17,18] while the 6 W belt and 3 W cap of the B isomer have edge-sharing octahedra (Figure 6B) which exhibit smaller $^2J_{W-O-W} \simeq 5-12$ Hz couplings.[17,18] Although the quadrupolar influence of the ^{51}V nuclei[18,19] broadens ($\Delta\nu_{1/2} \geq 4$ Hz in wet CD_3CN) the usually sharp ($\Delta\nu_{1/2} < 1$ Hz) ^{183}W resonances, a resolution-enhanced, two-line ^{183}W of $(Bu_4N)_4H_3SiW_9V_3O_{40}$ in wet CD_3CN reveals an apparent $^2J_{W-O-W}$ of about 15 Hz. Furthermore, the water-soluble free acid $H_7SiW_9V_3O_{40}$ was prepared by ion exchange of the K^+ salt and a ^{183}W NMR of a D_2O solution (ca. 2 g/mL of D_2O), Figure 7, exhibits sharper lines, and it clearly shows reciprocal couplings of 16.4 ± 1.2 Hz, confirming the A-type $SiW_9V_3O_{40}^{7-}$ structure.

(III) Deprotonation Studies. Preparation of $(Bu_4N)_{7-x}H_xSiW_9V_3O_{40}$ (x = 0–2). One of the primary goals of these studies was to prepare the fully deprotonated $(Bu_4N)_7SiW_9V_3O_{40}$ as a synthetic precursor for the support of transition-metal and organometallic catalysts. The mono- and diprotonated $H_xSiW_9V_3O_{40}^{x-7}$ (x = 1, 2) and especially their overall symmetry and sites of H^+ attachment (and their H^+ mobility with added H_2O or base) are also of interest since one might expect cationic metals to behave similarly. There is also the question of whether or not any $SiW_9V_3O_{40}^{7-}$ degradation by OH^- occurs along with removal of one, two, and three H^+.

Initially, the deprotonation of $(Bu_4N)_4H_3SiW_9V_3O_{40}$ in CH_3CN, Me_2SO, or DMF was surveyed by a potentiometric titration using $Bu_4N^+OH^-$ in MeOH or H_2O as titrant and a pH electrode and meter (millivolt scale) to monitor the titrations. In each solvent, sharp break points at 1.0 and 2.0 equiv of $Bu_4N^+OH^-$ were observed (Figure 2, supplementary material), but control experiments indicated that under our conditions, the electrode was unable to monitor the third equivalence point.[20] Monitoring the IR vs. equiv of $Bu_4N^+OH^-$ revealed a general decrease in energy for all of the heteropolytungstate vibrations upon deprotonation due to the buildup and delocalization[21] of negative charge. For example, the M=O vibration in CH_3CN decreased by approximately 20 cm^{-1} for $(Bu_4N)_7SiW_9V_3O_{40}$ compared to $(Bu_4N)_4H_3SiW_9V_3O_{40}$ (Figure 3, supplemental material).

The diprotonated $(Bu_4N)_5H_2SiW_9V_3O_{40}$ was prepared by addition of 1 equiv of $Bu_4N^+OH^-$/MeOH to $(Bu_4N)_4H_3SiW_9V_3O_{40}$ in CH_3CN followed by evaporation of the solvent to dryness under vacuum. ^{183}W and ^{51}V NMR studies in dry CD_3CN revealed broadened/multiple-line spectra that sharpened to averaged two (^{183}W) and one (^{51}V) line spectra with added H_2O, as anticipated on the basis of the earlier results for $H_3SiW_9V_3O_{40}^{4-}$. A summary of the ^{183}W and ^{51}V NMR data is provided in the Experimental Section.

(A) $(Bu_4N)_6HSiW_9V_3O_{40}$. Solid, dry samples of the monoprotonated salt $(Bu_4N)_6HSiW_9V_3O_{40}$ were prepared by addition of 2.0 equiv of $Bu_4N^+OH^-$/MeOH to a CH_3CN solution of the triprotonated salt followed by evaporation of the mixture to dryness under vacuum at room temperature. The ^{51}V and ^{183}W NMR at 21 °C of the product dissolved in dry CH_3CN results in strikingly clean and informative spectra, Figure 8. The ^{51}V NMR exhibits two resonances, one sharp resonance, δ −545 (1 V, $\Delta\nu_{1/2}$ = 106 Hz), and one broad resonance of relative intensity of approximately two, δ −578 (2 V, $\Delta\nu_{1/2}$ = 1871 Hz), requiring that $HSiW_9V_3O_{40}^{6-}$ possess a single mirror plane of symmetry (C_S symmetry). The substantially different line widths of the two ^{51}V resonances reflect the large difference in field gradient of the distinct vanadium sites upon protonation and suggest protonation of an oxygen bridging the two V responsible for the broad resonance, e.g., V_1–O(H^+)–V_2, Figure 9.

The ^{183}W NMR confirms the finding of overall C_S symmetry, since a five-line spectrum with resonances at −83.3, −88.1, −93.3,

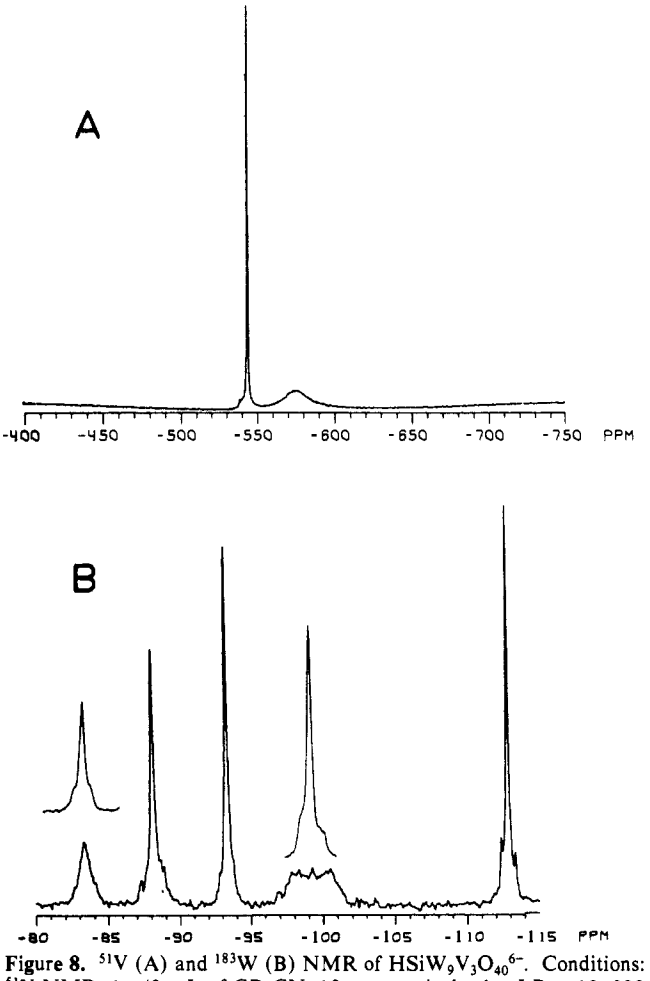

Figure 8. ^{51}V (A) and ^{183}W (B) NMR of $HSiW_9V_3O_{40}^{6-}$. Conditions: ^{51}V NMR, 1 g/3 mL of CD_3CN, 12-mm vertical tube, LB = 10, 200 transients, 0.04 min, 21 °C); ^{183}W NMR, 1 g/mL of CD_3CN, 10-mm vertical tube, LB = 1, 70 000 transients, 15.9 h. The inset peaks of (B) show the peak sharpening that results from 1.9-W decoupling of the −545 ppm ^{51}V resonance.

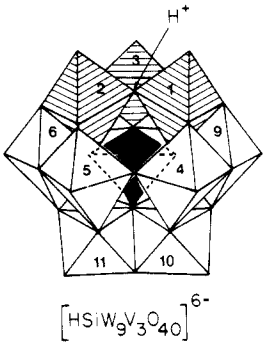

Figure 9. Polyhedral representation of A-β-$HSiW_9V_3O_{40}^{6-}$ illustrating the probable V_1–O(H)–V_2 protonation site.

(17) (a) Lefebrve, J.; Chauveau, F.; Doppelt, P.; Brevard, C. *J. Am. Chem. Soc.* **1981**, *103*, 4589. (b) Knoth, W. H.; Domaille, P. J.; Roe, D. C. *Inorg. Chem.* **1983**, *22*, 198. (c) Domaille, P. J.; Knoth, W. H. *Inorg. Chem.* **1983**, *22*, 818. (d) Brevard, C.; Schimpf, R.; Tourné, G.; Tourné, C. *J. Am. Chem. Soc.* **1983**, *105*, 7059.

(18) Domaille, P. J. *J. Am. Chem. Soc.* **1984**, *106*, 7677.

(19) Acerete, R.; Hammer, C. F.; Baker, L. C. W. *J. Am. Chem. Soc.* **1982**, *104*, 5384.

(20) (a) Control experiments indicated that the limit of the electrode's response under our experimental conditions was near the potential observed following 2.0 equiv of $Bu_4N^+OH^-$ (as shown on Figure 3, supplementary material). Some degradation of $SiW_9V_3O_{40}^{7-}$ (see text) also may have generated an interference as well.[20b] (b) Skoog, D. A.; West, D. M. "Principles of Instrumental Analysis"; Holt, Rinehart, Winston: New York, 1971; pp 450–459.

(21) Charge delocalization in polyoxoanions via a long M–O, short M=O, long M–O, and so on trans bond alternation ("cooperative trans influences") has been observed: (a) Besecker, C. J.; Day, V. W.; Klemperer, W. G.; Thompson, M. R. *Inorg. Chem.* **1985**, *24*, 44. (b) Besecker, C. J.; Day, V. W.; Klemperer, W. G.; Thompson, M. R. *J. Am. Chem. Soc.* **1984**, *106*, 4125. (c) Flynn, C. M., Jr.; Stucky, G. D. *Inorg. Chem.* **1969**, *8*, 335. (d) Day, V. W.; Fredrick, M. F.; Thompson, M. R.; Klemperer, W. G.; Liu, R.-S.; Shum, W. *J. Am. Chem. Soc.* **1981**, *103*, 3597. (e) Pope, M. T. *Inorg. Chem.* **1976**, *15*, 2008. (f) Pope, M. T.; Garvey, J. F. *Inorg. Chem.* **1978**, *17*, 1115.

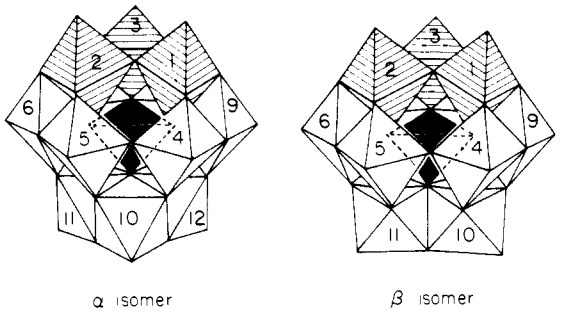

Figure 10. Polyhedral representations of α and β isomers of A-$HSiW_9V_3O_{40}^{6-}$ for illustrating the different connectivities resulting from imposition of C_S symmetry due to, for example, protonation of the V_1–O–V_2 bridging oxygen.

−99 (very broad), and −112.9 ppm of relative intensity 1:2:2:2:2 is observed. The very broad line at ca. −99 ppm and the partially broadened resonance at ca. −83 ppm are two additional interesting features of the ^{183}W NMR. Such broadened resonances have been observed previously for vanadotungstates and are attributed to the scalar relaxation of ^{183}W caused by quadrupolar relaxation of ^{51}V.[18,19] The broad ^{51}V line has little effect on the ^{183}W NMR spectrum because the rapid relaxation self-decouples it from the adjacent tungstens. On the other hand, the more slowly relaxing, sharper ^{51}V line broadens both the ^{183}W resonance of the adjacent pair of tungstens (−99 ppm) and the unique tungsten which is *four bonds removed* (−83 ppm). Consistent with the above interpretation, decoupling of the sharper ^{51}V resonance results in a marked narrowing of the broadened ^{183}W resonance centered at −99 ppm (Figure 8B). We have also quantified the vanadium–tungsten couplings from fitting the line shapes using established theory.[18] The measured T_1 value of the sharper ^{51}V resonance is 9.5 ms in the same solution used to obtain the ^{183}W NMR spectrum. Line shape calculations, which are quite sensitive to the magnitude of the J values, give $^2J_{V\text{-}O\text{-}W} = 10.5 \pm 0.5$ Hz for the broad ^{183}W line at −99 ppm and $^4J_{V\text{-}O\text{-}W} = 4.0 \pm 0.5$ Hz for the line at −83 ppm. The large magnitude of the latter four-bond coupling is a surprising and potentially important result, one that issues a warning that tungsten–tungsten couplings of a similar magnitude may be observable over such large distances. If more general, the observation of four-bond couplings might limit the use of tungsten–tungsten couplings in establishing connectivities, since adjacent two-bond couplings for edge-shared tungsten are typically 5–12 Hz. Why the four-bond vanadium–tungsten coupling is observed for $HSiW_9V_3O_{40}^{6-}$ is not obvious in the absence of an X-ray crystallographic structure determination. Since $^2J_{W\text{-}O\text{-}W}$ and $^2J_{V\text{-}O\text{-}W}$ couplings increase as the M–O–M angle increases toward 180°,[17,18] a possible explanation is that protonation causes a flattening of one or more M–O–M (M = V, W) angles.

The use of 2-D ^{183}W NMR allows us to answer the final structural question about A-$SiW_9V_3O_{40}^{7-}$, namely, whether the β isomerism[10] of the A-β-$SiW_9O_{34}^{10-}$ starting material is retained in the A-$SiW_9V_3O_{40}^{7-}$ product. As evident in Figure 10, differences in the mode of W–W connectivity are apparent for the α vs. β isomer of C_S symmetry $SiW_9V_3O_{40}^{7-}$. The 2-D INADEQUATE pulse sequence[22] allows detection of each pair of low abundance, coupled satellite doublets and has already proven powerful in unambiguously establishing the atomic framework of heteropolytungstates.[17b–d,18a,23] The ^{51}V-decoupled 2-D INADEQUATE ^{183}W NMR of $(Bu_4N)_6HSiW_9V_3O_{40}$ in dry CD_3CN is shown in Figure 11, with the data presented as a contour plot; the 1-D $^{183}W\{^{51}V\}$ spectrum is presented below it on the same scale. The

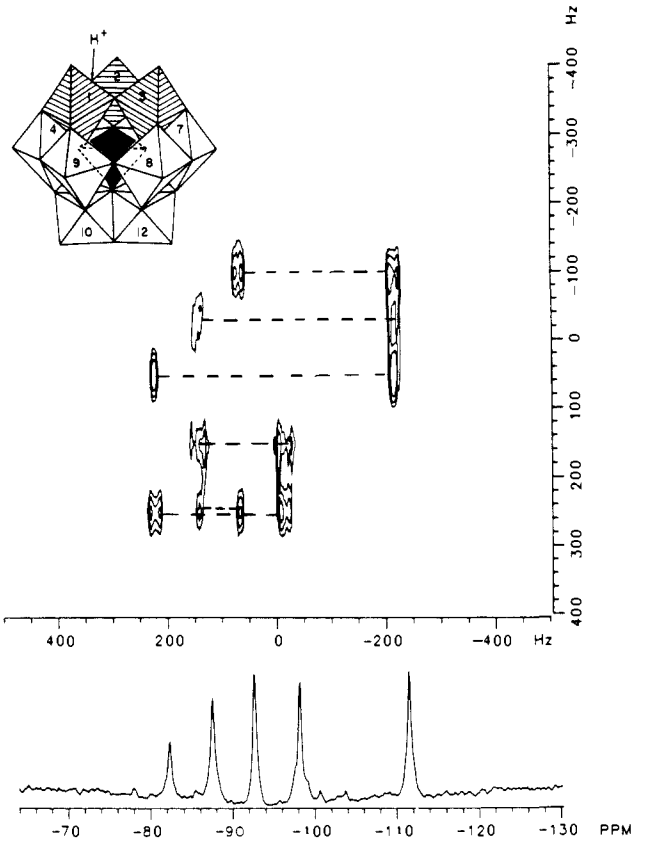

Figure 11. Contour plot of the $^{183}W\{^{51}V\}$ NMR 2-D INADEQUATE spectrum for A-β-$HSiW_9V_3O_{40}^{6-}$ using a 20-mm sideways-spinning probe at 30 °C. The bottom spectrum is of the 1-D ^{183}W NMR with 1.9-W decoupling of the −545 ppm resonance in the ^{51}V NMR. Connectivities between ^{183}W resonances are indicated by dashed lines. Corner couplings appear as "dumbbells" while edge couplings appear as "single ovals". For a discussion of the tungsten octahedral connectivities (according to the labeling scheme indicated) see the text.

complete connectivity pattern can be accounted for *only* with the β isomer and the assignment −82.5 (W_{12}), −87.7 (W_6, W_9), −92.8 (W_4, W_5), −98.3 (W_7, W_8), and −111.7 ppm (W_{10}, W_{11}).[24] This assignment is made, step-by-step, from the contour 2-D plot, Figure 11, starting with the unique tungsten (W_{12} for the β isomer). The spectrum reveals both a W_{12}–$W_{7,8}$ corner and a W_{12}–$W_{10,11}$ edge connectivity. Similarly, a $W_{7,8}$–$W_{6,9}$ corner, a $W_{6,9}$–$W_{5,4}$ edge and a $W_{6,9}$–$W_{10,11}$ corner, and a $W_{5,4}$–$W_{10,11}$ corner coupling are apparent, thereby unequivocally establishing the structure as β-$SiW_9V_3O_{40}$, Figure 10.

Although the C_S symmetry, A-β structure of $HSiW_9V_3O_{40}^{6-}$ is unequivocally established by the ^{51}V and 1- and 2-D ^{183}W NMR, the site of protonation is not. However, the ^{51}V NMR line widths (vide supra) are most consistent with H^+ addition to an oxygen-bridging V_1 and V_2, i.e. V_1–$(OH)^+$–V_2 (Figure 10). Furthermore, the ESR studies by Pope et al.[6b] of the 1-e^--reduced $HSiW_9V_2V^{IV}O_{40}^{7-}$ also favored protonation of a V_2O site and Klemperer et al. determined by ^{17}O NMR that V_2O protonation occurs in[25a] $HV_2W_4O_{19}^{3-}$ and that V_2O plus some V_3O protonation occurs in[25b,c] $V_{10}O_{28}^{6-}$. The IR of $(Bu_4N)_6HSiW_9V_3O_{40}$ vs. that

(22) (a) Bax, A. "Two-Dimensional NMR in Liquids"; Delft University Press: 1982. (b) Bax, A.; Kempsell, S. P.; Freeman, R. *J. Magn. Reson.* **1980**, *41*, 349. (c) Bax, A.; Freeman, R.; Frenkiel, T. A.; Levitt, M. H. *Ibid.* **1981**, *43*, 478.

(23) In fact, it is already quite clear that chemical shift assignments made in the absence of the connectivity data obtainable by 2-D ^{183}W NMR and $^2J_{W\text{-}O\text{-}W}$ couplings are likely to be in error. See, for example, the discussion and references in ref 18.

(24) If one tries to assign the 2-D ^{183}W NMR in Figure 11 to the α isomer using its tungsten numbering scheme as shown in Figure 10, the intensity-one resonance would have to be W_{10} and its corner coupling to the peak at −99 ppm would assign the latter resonance to $W_{4,5}$. Next, a $W_{4,5}$–$W_{6,9}$ edge coupling would be required. However, one is not present in the 2-D spectrum which rapidly illustrates, in part, how the α isomer was ruled out. Additionally, the four-bond vanadium–tungsten coupling to the unique, intensity-one tungsten assigned to V_3–W_{12} ($^4J_{V_3\text{-}O\text{-}W_{12}}$) in the β isomer would be an untenable, ≥six bond $^6J_{V_3\text{-}W_{10}}$ in the α isomer.

(25) (a) Klemperer, W. G.; Shum, W. *J. Am. Chem. Soc.* **1978**, *100*, 4891; (b) *J. Am. Chem. Soc.* **1977**, *99*, 3544. (c) Evans, H. T., Jr.; Pope, M. T. *Inorg. Chem.* **1984**, *23*, 501. See also: Harrison, A. T.; Howarth, O. W. *J. Chem. Soc., Trans.* **1985**, 1953.

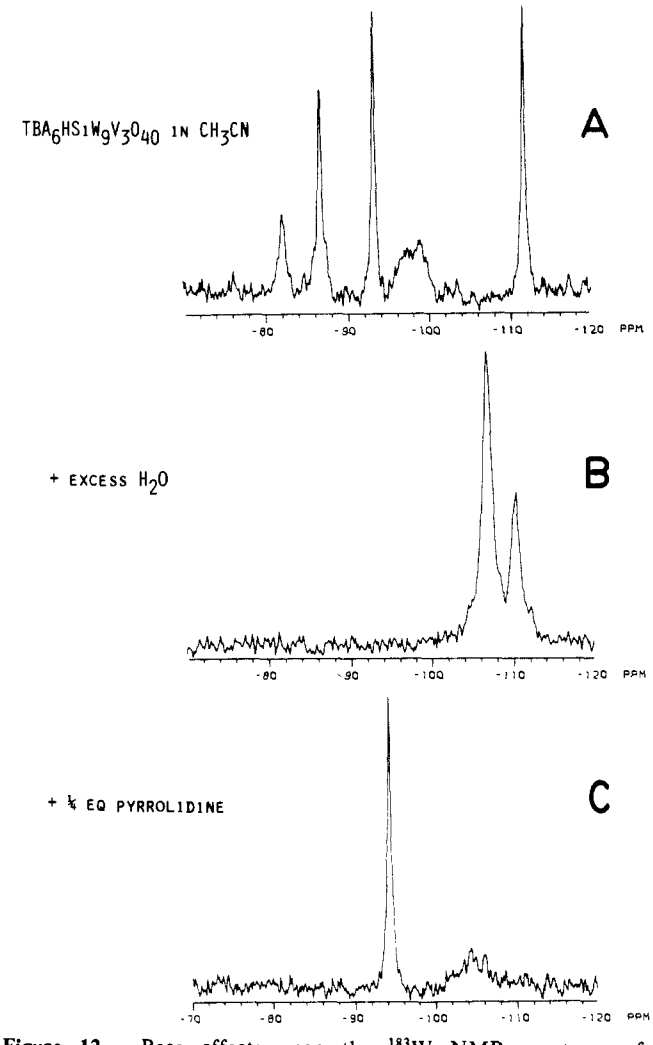

Figure 12. Base effects upon the ^{183}W NMR spectrum of $(Bu_4N)_6HSiW_9V_3O_{40}$. (A) $(Bu_4N)_6HSiW_9V_3O_{40}$ (1 g/2 mL of CD_3CN, 10-mm vertical tube, LB = 2, 10000 transients, 2.3 h, 21 °C). (B) (A) in the presence of a large excess of water (10-mm vertical tube, LB = 2, 35000 transients, 8 h, 21 °C). (C) Sample (A) plus $^1/_4$ equiv of pyrrolidine (1 g/2 mL of CD_3CN plus 5.3 μL of pyrrolidine, LB = 2, 20000 transients, 4.6 h, 21 °C).

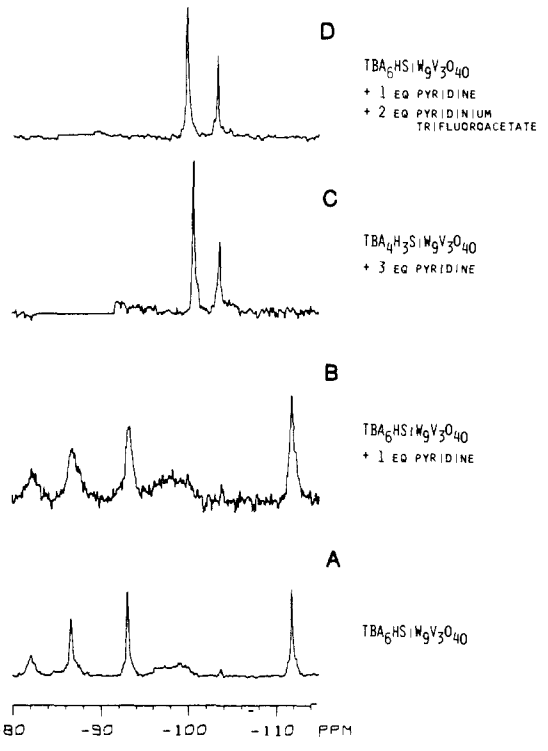

Figure 13. Effects of pyridine upon protonated A-β-$SiW_9V_3O_{40}^{7-}$ as monitored by ^{183}W NMR. From bottom to top the spectra are of (A) A-β-$(Bu_4N)_6HSiW_9V_3O_{40}$ in CD_3CN alone (2 g/3 mL of 3:1 DMF/CD_3CN, 10-mm vertical tube, LB = 1, 40000 transients, 9.1 h, 21 °C), (B) sample (A) following the addition of 1 equiv of pyridine (41 μL) (LB = 2, 40000 transients, 9.1 h, 21 °C), (C) $(Bu_4N)_4H_3SiW_9V_3O_{40}$ plus 3 equiv of pyridine (2 g of sample/3 mL of 3:1 DMF/CD_3CN plus 141 μL of pyridine, LB = 1, 70000 transients, 15.9 h, 21 °C), and (D) sample (B) following the addition of 2 equiv, 197 mg, of pyridinium trifluoroacetate (LB = 1, 70000 transients, 15.9 h, 21 °C).

of $(Bu_4N)_7SiW_9V_3O_{40}$ in CH_3CN (and $(Bu_4N)_5H_2SiW_9V_3O_{40}$ and $(Bu_4N)_4H_3SiW_9V_3O_{40}$; Figure 3, supplementary material) is also consistent with protonation of predominantly a V_2O site.[26]

The finding of proton localization on the NMR time scale in $HSiW_9V_3O_{40}^{6-}$ and elucidation of V_2O as a probable protonation site offers the opportunity to examine the H^+ mobility induced by added H_2O or other bases in greater detail. As shown in Figure 12, (excess) H_2O causes collapse of the five-line C_S symmetry ^{183}W NMR spectrum to a two-line, 2:1 intensity C_{3v} (average) spectrum. Use of only 0.25 equiv of the stronger base pyrrolidine [pK_b = 2.7 (25 °C)] is even more effective at collapsing the five-line spectrum to a sharp, two-line spectrum (Figure 12C), results that rule out complete deprotonation to $SiW_9V_3O_{40}^{7-}$ as an explanation for the two-line, C_{3v} symmetry spectrum. Studies with the weaker base pyridine [pK_b = 8.8 (25 °C)] offer additional insights, Figure 13. While 1 equiv of pyridine added to $HSiW_9V_3O_{40}^{6-}$ causes only partial collapse of the five-line spectrum, the addition of 3 equiv of pyridine to $H_3SiW_9V_3O_{40}^{4-}$ causes full collapse to a sharp, two-line spectrum. Both these experiments were expected to generate $HSiW_9V_3O_{40}^{6-}$ in the presence of 1 equiv of pyridine, except that the latter reaction, $H_3SiW_9V_3O_{40}^{4-}$ + 3 equiv of py, *also produces 2 equiv of pyH*$^+$. As a check, 2 equiv of pyH^+-$CF_3CO_2^-$ along with 1 equiv of py was added to $HSiW_9V_3O_{40}^{6-}$ and, indeed, a sharp two-line ^{183}W NMR spectrum was observed, Figure 13D. These results require that in addition to a deprotonation/reprotonation mechanism, $HSiW_9V_3O_{40}^{6-}$ + py ⇌ [$SiW_9V_3O_{40}^{7-}$ + pyH^+] ⇌ $HSiW_9V_3O_{40}^{6-}$ + py, a protonation/deprotonation mechanism also is operative, pyH^+ + $HSiW_9V_3O_{40}^{6-}$ ⇌ [py + $H_2SiW_9V_3O_{40}^{5-}$] ⇌ pyH^+ + $HSiW_9V_3O_{40}^{6-}$. The net result is py- *and* pyH^+-assisted H^+ mobility over the three V–O–V sites of the V_1, V_2, and V_3 (Figure 10) triad of VO_6 octahedra in $SiW_9V_3O_{40}^{7-}$. Only a few previous studies of protonation in polyoxoanions exist,[25] and the present studies constitute the best homogeneous model for H_2O-, base-, and base-H^+-assisted H^+ mobility on heterogeneous, M_xO_y oxide surfaces. Additional studies such as the rate and rate law to quantify the H^+-exchange processes are needed, however.

(B) $(Bu_4N)_7SiW_9V_3O_{40}$. For the synthesis of surface-attached transition metals or organometallics, complete deprotonation to $SiW_9V_3O_{40}^{7-}$ and its isolation are required. $(Bu_4N)_7SiW_9V_3O_{40}$ was prepared analogously to the other deprotonated species, by 3 equiv of $Bu_4N^+OH^-$/MeOH addition to $(Bu_4N)_4H_3SiW_9V_3O_{40}$ followed by removal of the solvent under vacuum at room temperature. ^{51}V and ^{183}W NMR in comparison to that for $HSiW_9V_3O_{40}^{6-}$, Figure 14B, and C, respectively, show that, in addition to the anticipated two-line, 2:1 intensity spectrum for C_{3v} $SiW_9V_3O_{40}^{7-}$, some $HSiW_9V_3O_{40}^{6-}$ remains. Moreover, in the more sensitive ^{51}V NMR, several additional peaks are present (Figure 14). In a sample prepared with 1.0 additional equiv of $Bu_4N^+OH^-$/MeOH (i.e., 4.0 equiv of $Bu_4N^+OH^-$/MeOH + $(Bu_4N)_4H_3SiW_9V_3O_{40}$ followed by vacuum removal of the solvent,

(26) Some protonation of the three bridging oxygen, C_S symmetry site provided by the $V_1W_4W_9$ triad might be expected since it is this site in $[CpTi{\cdot}SiW_9V_3O_{40}]^{2-}$[1b,c] and the analogous $Nb_1W_4O_9$ site in $[(C_5Me_5)Rh{\cdot}SiW_9Nb_3O_{40}]^{3-}$[1a] where the $CpTi^{3+}$ and $(C_5Me_5)Rh^{2+}$ organometallic units are thought to bind (on the basis of their five-line, C_S symmetry ^{183}W NMR spectra and, especially, their 35- and 30-cm^{-1} splittings, respectively, of the 800-cm^{-1} edge-sharing M–O–M vibration). In $HSiW_9V_3O_{40}^{6-}$ vs. $SiW_9V_3O_{40}^{7-}$ there is little splitting of this band, suggesting less sterically hindered electrophiles like H^+ prefer the probably more basic V_2O site.

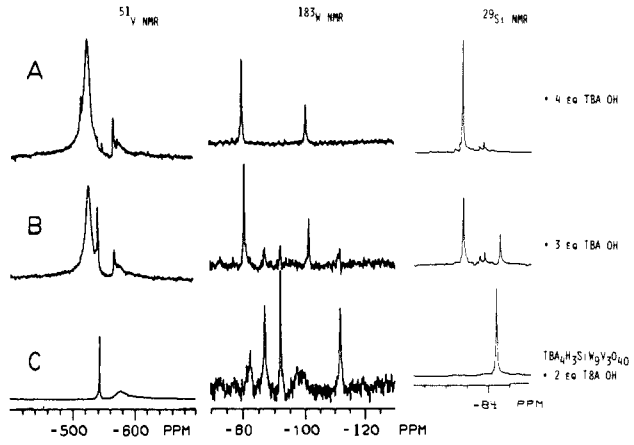

Figure 14. NMR study of the deprotonation of $(Bu_4N)_6HSiW_9V_3O_{40}$ (prepared from $(Bu_4N)_4H_3SiW_9V_3O_{40}$ plus 2 equiv of $Bu_4N^+OH^-$) as monitored by ^{51}V NMR (left), ^{183}W NMR (center), and ^{29}Si NMR (right) as a function of 0 added equiv of $Bu_4N^+OH^-$ (C), 1 added equiv of $Bu_4N^+OH^-$ (B), and 2 added equiv of $Bu_4N^+OH^-$ (A). Conditions: ^{51}V NMR, 1 g/2 mL of CD_3CN, 12-mm vertical tube, LB = 25, 200 transients, 0.04 min, 21 °C; ^{29}Si NMR, 2 g/2 mL of CD_3CN, 12-mm vertical tube, LB = 1, 8000 transients, 2.8 h, 21 °C; ^{183}W NMR, 2 g/2 mL of CD_3CN, 10-mm vertical tube, LB = 2, 3000 transients, 0.7 h, 21 °C. See the Experimental Section for details concerning such deprotonations.

Figure 14A), the residual $HSiW_9V_3O_{40}^{6-}$ is gone and the ^{183}W NMR spectra appears clean but the more sensitive ^{51}V NMR shows, in fact, that complete deprotonation of $H_3SiW_9V_3O_{40}^{4-}$ is accompanied by approximately 23% (by ^{51}V NMR) to 29% (by ^{29}Si NMR) decomposition.[27] This decomposition does not hinder the synthesis of cyrstalline, analytically pure $(Bu_4N)_4[CpTiSiW_9V_3O_{40}]$ from $CpTi^{3+}$ and $SiW_9V_3O_{40}^{7-}$, however,[1b,c] but it does reduce the yield and does show that one must demonstrate, and not assume, complete deprotonation without decomposition of polyoxoanions solubilized in organic media.

(IV) $H_xP_2W_{15}V_3O_{62}^{x-9}$. Since a simple, high-yield, single-step synthesis to $P_2W_{15}V_3O_{62}^{9-}$ had not been previously reported,[6b] we undertook its synthesis as a test of the straightforward, successful route used in preparing $H_3SiW_9V_3O_{40}^{4-}$. The Bu_4N^+ salt $(Bu_4N)_{9-x}H_xP_2W_{15}V_3O_{62}$ and its deprotonation are also of interest, since the anticipated structure of $(Bu_4N)_9P_2W_{15}V_3O_{62}$ is the trivanadium-substituted C_{3v} symmetry anion with a B-type triad of edge-sharing VO_6 octahedra, Figure 2B. As such, it provides a B-type site for support of organometallic fragments, such as $CpTi^{3+}$, for example,[1b,c] providing a comparison with the A-type support site on $(Bu_4N)_7SiW_9V_3O_{40}$.

(A) Synthesis and Characterization of the $(Me_4N)_6^{6+}$ and K_8^{8+} Salts. The desired reaction proceeded smoothly as anticipated, providing the orange Me_4N^+ salt on a ca. 10-g scale in 80% recrystallized yield:

$$Na_{12}P_2W_{15}O_{56} + 3NaVO_3 + 9HCl \xrightarrow[\text{2. hot, pH 1.5 water recrystallization in 80\% yield}]{\text{1. } Me_4N^+Cl^- \text{ to ppt}} (Me_4N)_6H_3P_2W_{15}V_3O_{62}\cdot 6H_2O$$

The Me_4N^+ product has been characterized by elemental analysis, solution molecular weight, TGA, and ^{31}P, ^{51}V, ^{183}W, and 2-D ^{183}W NMR methods. The analytical data sets the empirical formula at $[(Me_4N)_6P_2W_{15}V_3O_{ca.\,62}]_n$ and the molecular formula of $H_xP_2W_{15}V_3O_{62}^{x-9}$ was established by conventional methods, since FABMS at $m/z >$ ca. 4000 has only recently become available.[9b] The solution molecular weight in water, as determined by the sedimentation equilibrium method, confirms the presence of a monomer, $n = 1$ (calcd for $P_2W_{15}V_3O_{62}^{9-}$, 3965; found 3622; Figure 1B, supplemental materials). The IR data for the anion $H_xP_2W_{15}V_3O_{62}^{x-9}$, tabulated in the Experimental Section for the representative K^+ salt, is consistent with the Wells–Dawson (i.e., $P_2W_{18}O_{62}^{6-}$) structure and is essentially identical with the spectrum reported for the 1-e$^-$-reduced V^{IV}, analogue.[6b] The combined data are fully supportive of a $(Me_4N)_6H_{3-x}(H_3O)_xP_2W_{15}V_3O_{62}$ formulation, with three protons (hydronium ions) as required by charge balance. It is interesting to note that a simple change from Me_4N^+ to K^+ while keeping the pH constant gives the crystalline K_8^{8+} salt as compared to the $Me_4N_6^{6+}$ salt. (See the data in the Experimental Section.) These results issue a warning against extrapolating, without independent evidence, polyoxoanion salt compositions from one cation to even closely related cations.

The ^{51}V, ^{31}P, and ^{183}W NMR data for $D_xP_2W_{15}V_3O_{62}^{x-9}$ in D_2O (where rapid D^+ mobility can occur) confirm the previously established[6b] C_{3v} average symmetry structure. The ^{51}V NMR of the (more soluble) Li^+ salt, prepared by ion exchange from the K^+ salt, shows a single resonance at −504 ppm [$\Delta\nu_{1/2}$ = 110 Hz, pD 6.3 (from pH(apparent) 5.9),[28a] 30 °C]. The high-sensitivity ^{31}P NMR spectrum, Figure 15 (lower spectrum, inset), shows only (≥98%) two types of phosphorus resonances, expected for $H_xP_2W_{15}V_3O_{62}^{x-9}$, thereby confirming the homogenity of the sample. The PO_4^{3-} group connected to the tungstens labeled B

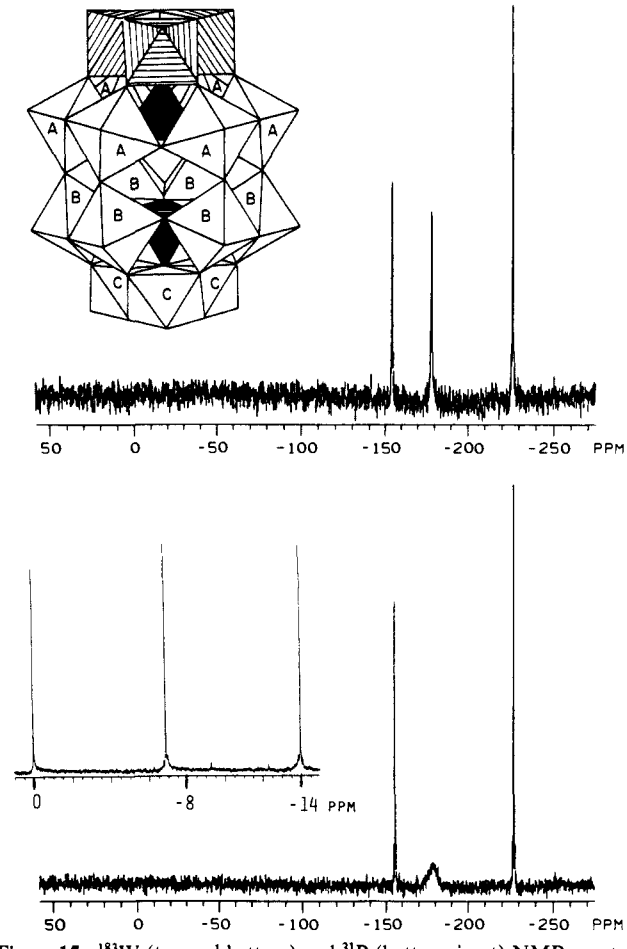

Figure 15. ^{183}W (top and bottom) and ^{31}P (bottom, inset) NMR spectra of $D_xP_2W_{15}V_3O_{62}^{x-9}$, prepared following the metathesis of the Me_4N^+ salt to the Li^+ salt at pD 6.3 D_2O, 30 °C, 20-mm sideways-spinning tube. The bottom spectrum is the ^{183}W NMR without ^{51}V decoupling; the upper spectrum was taken with 4.5-W ^{51}V decoupling. In the ^{31}P NMR, 85% H_3PO_4/H_2O was introduced via a concentric tube, resulting in the line at 0 ppm.

(27) As a control, $Bu_4N^+OH^-$ in water instead of MeOH was used for the 1.0, 2.0, and 3.0 equiv of OH^- deprotonation of $(Bu_4N)_4H_3SiW_9V_3O_{40}$ as monitored by ^{51}V NMR. Identical results with the $Bu_4N^+OH^-$/MeOH experiments were obtained up to and including 2.0 equiv, but with >2.0 equiv and even greater number of ^{51}V NMR resonances are observed suggesting, not unexpectedly, that H_2O aids the decomposition of $SiW_9V_3O_{40}^{7-}$.

(28) (a) The pD was calculated from the measured pH(apparent) by pD = pH + 0.4: Glasoe, P. K.; Long, F. A. *J. Phy. Chem.* **1960**, *64*, 188. (b) Massart, R.; Contant, R.; Fruchart, J. M.; Ciabrini, J. P.; Fournier, M. *Inorg. Chem.* **1977**, *16*, 2916.

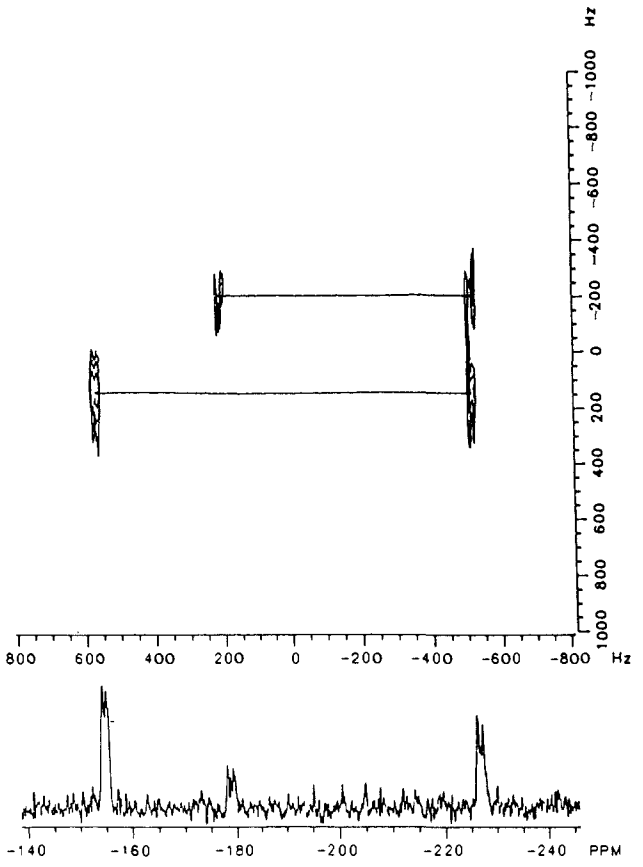

Figure 16. $\{^{51}V\}^{183}W$ 2-D INADEQUATE spectrum of $P_2W_{15}V_3O_{62}^{9-}$, prepared following the metathesis of the Me_4N^+ salt to the Li^+ salt at pD 6.3 D_2O, 30 °C, 20-mm sideways-spinning tube.

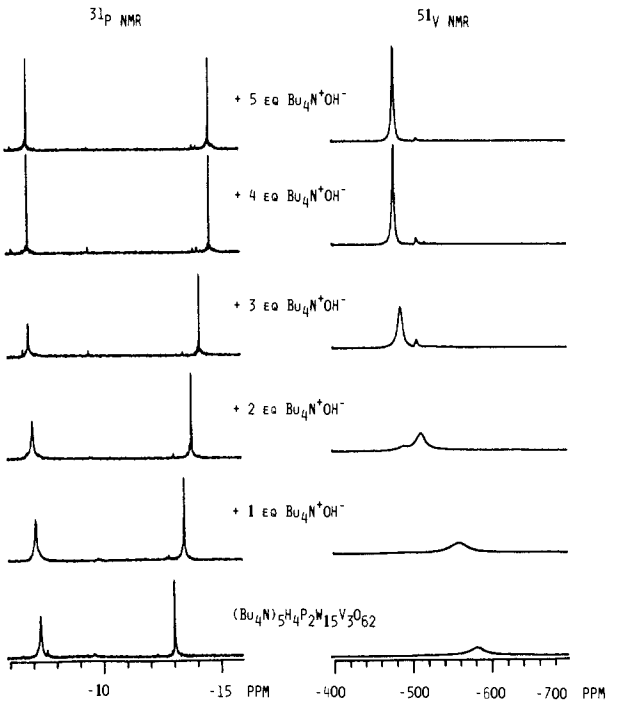

Figure 17. Deprotonation of $(Bu_4N)_5H_4P_2W_{15}V_3O_{62}$ as monitored by ^{31}P (left) and ^{51}V (right) NMR spectroscopy with $Bu_4N^+OH^-$/water. Conditions: ^{31}P NMR, 0.032 M 1:1 CH_3CN/CD_3CN, 12-mm vertical tube, LB = 0.5, 64 transients, 2.2 min, 21 °C; ^{51}V NMR, 0.032 M 1:1 CH_3CN/CD_3CN, 12-mm vertical tube, LB = 5, 600 transients, 0.12 min. See the Experimental Section for details concerning such deprotonations.

and adjacent to the W_3 cap (see Figure 15 inset) is assigned to the high-field line at −14 ppm by comparison to the similar chemical shift found for a PO_4^{3-} in the similar environment provided by α-$P_2W_{18}O_{62}^{6-}$ (δ −12.7).[28b] The PO_4^{3-} group connected to the tungstens labeled A and to the V_3 cap (see Figure 15 inset) is then assigned to the downfield, δ −6.9, resonance, consistent with the chemical shifts in substituted heteropolytungstates.[1f,6b,28b] The ^{183}W NMR and the $^{183}W\{^{51}V\}$ NMR spectra for $D_xP_2W_{15}V_3O_{62}^{x-9}$ in D_2O, Figure 15 (lower and upper spectra, respectively), show the three resonances of 2:2:1 intensity expected for the tungsten "belts" a and b of 6 W and a tungsten cap of 3 W, Figure 15, inset. The very broad −226.7 ppm (6 W, $\Delta\nu_{1/2}$ = 54 Hz) sharpens with ^{51}V decoupling (Figure 15, upper spectrum), indicating an assignment of that resonance to the six a-type tungstens closest to the vanadium cap, although complete decoupling, which would have allowed observation of the satellite $^2J_{W\text{-}O\text{-}W}$ and therefore unambiguous assignments of the ^{183}W NMR, could not be obtained due to limitations in the decoupling power available. However, a $^{183}W\{^{51}V\}$ 2-D INADEQUATE NMR spectrum, Figure 16, shows the intensity-one resonance, c, at ca. −158 ppm is (corner) coupled to the ca. −227 resonance, hence the assignment of the −227 line to the six belt tungsten resonance, type b. A single (corner) coupling of the −227 ppm, W type b, resonance to the −179 ppm, 6 W type a resonance, completes the assignments and confirms the structure shown (Figure 15, inset). Given the present limited understanding and hence unpredictability of ^{183}W NMR chemical shifts (such as the downfield location of the $6W_a$ vs. $6W_b$), the significance of $^2J_{W\text{-}O\text{-}W}$ couplings and of 2-D NMR techniques in making unambiguous chemical shift assignments is again apparent.[17,18,23]

(B) Synthesis and Characterization of $(Bu_4N)_{9-x}H_xP_2W_{15}V_3O_{62}$. As a rule, we monitor even such simple reactions as metathetical exchanges by NMR (such as ^{31}P NMR). Even so, it was surprising that initial attempts at $Bu_4N^+Br^-$ or $(n\text{-}C_3H_7)_4N^+Br^-$ metathesis of either the (initially clean by ^{31}P NMR) Me_4N^+ or K^+ salts of $H_xP_2W_{15}V_3O_{62}^{x-9}$, followed by workup in an analogous fashion to that successfully utilized for $(Bu_4N)_4H_3SiW_9V_3O_{40}$ (a rapid MeOH wash and air drying followed by crystallization from $DMF/CHCl_3$) produced multiple lines in the ^{31}P NMR (CD_3CN solvent). This unexpected result from a "simple" metathetical exchange reaction illustrates the value of direct monitoring (e.g., ^{31}P or ^{51}V NMR) of each step in a polyoxoanion synthesis. The ^{31}P NMR lines did not collapse to a single pair of resonance following the addition of Br_2, indicating that reduced forms of $H_xP_2W_{15}V_3O_{62}^{x-9}$ were not involved, or following the addition of an excess of either H_2O or OH^-, indicating that multiple protonation or protonation at inequivalent sites on the anion was not responsible. Additional controls and ^{51}V NMR studies led to the discovery that $H_xP_2W_{15}V_3O_{62}^{x-9}$ apparently reacts irreversibly with MeOH, possibly forming V–OMe bonds. This sensitivity to MeOH stands in marked contrast to the insensitivity observed for $(Bu_4N)_4H_3SiW_9V_3O_{40}$ and issues a warning on the $MeOH/Et_2O$ drying step.[29]

A successful synthesis of the organic solvents soluble $(Bu_4N)_5H_4P_2W_{15}V_3O_{62}$ in nearly quantitative yield can be accomplished by metathesis of $K_8HP_2W_{15}V_3O_{62}$ with excess $Bu_4N^+Br^-$ in pH 1.5 water, followed by passing the product through a cation-exchange resin charged in the Bu_4N^+ form (to remove residual K^+ that results from an apparent incomplete metathetical exchange; see the Experimental Section) and reprecipitation of the $5Bu_4N^+$ salt[30] in pH 1.5 water (to remove any $Bu_4N^+Br^-$). The Bu_4N^+/polyoxoanion ratio was determined by both elemental C, H, N analysis and thermal gravimetric analysis to yield the formula[31] $(Bu_4N)_5H_4P_2W_{15}V_3O_{62}\cdot XH_2O$ ($X \leq 2$). The

(29) Rocchiccioli-Deltcheff, C.; Fournier, M.; Franck, R.; Thouvenot, R. *Inorg. Chem.* **1983**, *22*, 207. This paper provides many experimental tips for preparative polyoxoanion chemistry.

(30) While following the procedure outlined in the Experimental Section, in one instance a $[(Bu_4N)_6H_3]^{9+}$ (vs. the $[(Bu_4N)_5H_4]^{9+}$) salt was obtained (see Experimental Section). The use of TGA and/or C, H, N analysis for each preparation is recommended until such time as additional experiments, designed to yield a constant Bu_4N^+/H^+ ratio, are successful.

sensitive ^{31}P and ^{51}V NMR spectra of this Bu_4N^+ salt possess only the number of resonances expected for the C_{3v} symmetry α-1,2,3-trivanadium-substituted heteropolytungstate and as previously determined for the tetramethylammonium salt. However, both the ^{51}V and ^{31}P NMR are considerably broadened with respect to its tetramethylammonium analogue in water—a broadening that decreases markedly upon the addition of excess (100 equiv) water, analogous to the phenomena observed for $(Bu_4N)_4H_3SiW_9V_3O_{40}$ (and likewise attributed to a fast-averaging of the protons attached to the heteropolyanion's surface).

(C) Deprotonation of $(Bu_4N)_5H_4P_2W_{15}V_3O_{62}$. Figure 17 illustrates the changes that result in the ^{51}V and ^{31}P NMR as a result of the addition of successive equivalents of $Bu_4N^+OH^-$ to $(Bu_4N)_5H_4P_2W_{15}V_3O_{62}$. The significant features of these deprotonations are as follows. First, continuous chemical shift changes in the ^{51}V and ^{31}P NMR spectra occur when up to, *but not beyond*, 4 equiv of OH^- are added. This not only confirms the presence of a $H_4P_2W_{15}V_3O_{62}^{5-}$ anion but also indicates that all four protons are, in all probability, attached to the surface of the heteropolytungstate, as removal of a simple H_3O^+ counterion should have a negligible effect upon the compound's ^{31}P and ^{51}V NMR chemical shifts. Second, until 4 equiv of $Bu_4N^+OH^-$ are added, the ^{31}P and ^{51}V NMR remain broad, indicating the presence of a protonated heteropolyanion as presented earlier for $(Bu_4N)_4H_3SiW_9V_3O_{40}$. However, the broadened ^{31}P and ^{51}V NMR spectra for $HP_2W_{15}V_3O_{62}^{8-}$ in the absence of H_2O or added bases stands in marked contrast to the sharp ^{29}Si and ^{51}V NMR spectra observed for $HSiW_9V_3O_{40}^{6-}$ under similar conditions. Such a result, indicating tighter H^+ binding for $SiW_9V_3O_{40}^{7-}$ as compared to $P_2W_{15}V_3O_{62}^{9-}$, is consistent with the reported pK_a of 10.5 for $K_6HSiW_9V_3O_{40}$ as compared to a pK_a of 9 for the *one-electron-reduced* (and presumably even more basic) $K_9HP_2W_{15}V_3O_{62}$.[6] Third, the ^{31}P and ^{51}V NMR spectra of $P_2W_{15}V_3O_{62}^{9-}$ in the presence of additional OH^- show no evidence of decomposition, again in contrast to the results for $SiW_9V_3O_{40}^{7-}$, where removal of the final proton with OH^- was inevitably accompanied by some heteropolyanion decomposition. These results suggest that reaction of organometallic species with $P_2W_{15}V_3O_{62}^{9-}$ may be cleaner and/or occur in higher yield than its corresponding reaction with impure (or OH^- contaminated) $SiW_9V_3O_{40}^{7-}$.

Summary

The following list summarizes the major findings resulting from these studies:

(1) The straightforward, reasonable-yield syntheses of A-β-$H_xSiW_9V_3O_{40}^{x-7}$ and of $H_xP_2W_{15}V_3O_{62}^{x-9}$, including their previously unknown organic medium soluble Bu_4N^+ salts.

(2) The characterization of the products by elemental analysis, TGA, FABMS (for $K_6HSiW_9V_3O_{40}$), solution molecular weight measurements, IR, and ^{31}P, ^{29}Si, ^{51}V, ^{183}W, $^{183}W\{^{51}V\}$, and 2-D ^{183}W NMR. The results unambiguously demonstrate that the A-β structure of the A-β-$SiW_9O_{34}^{10-}$ lacunary precursor is retained in the A-β-$SiW_9V_3O_{40}^{7-}$ product. The results with $P_2W_{15}V_3O_{62}^{9-}$ unambiguously demonstrate that the three vanadiums occupy adjacent, edge-sharing positions in the cap as shown in Figure 2B thereby confirming the earlier structural findings of Harmalker, Leparulo, and Pope based on ESR and ^{31}P and ^{51}V NMR studies. The results strongly suggest, but do not prove, that the lacunary $P_2W_{15}O_{56}^{12-}$ precursor[32] has a structure with these three positions vacant.

(3) The first study of the stepwise deprotonation of the heteropolyanions $H_3SiW_9V_3O_{40}^{4-}$ and $H_4P_2W_{15}V_3O_{62}^{5-}$ in organic solvents, including documentation of the effects of protonation, dry vs. wet solvents, added bases upon the ^{29}Si, ^{31}P, ^{51}V, and ^{183}W NMR, and the base stability of these deprotonated, trisubstituted heteropolytungstates.

(4) The finding that fully deprotonated $P_2W_{15}V_3O_{62}^{9-}$ can be prepared without decomposition but that decomposition of $SiW_9V_3O_{40}^{7-}$ occurs, demonstrating that deprotonation without decomposition of Bu_4N^+ salts of polyoxoanions in organic solvents must be proven and not assumed in each case of interest.

(5) The elucidation of the C_S symmetry structure of $HSiW_9V_3O_{40}^{6-}$ and evidence that a V_2O, bridging oxygen site is the probable protonation site.

(6) The H_2O-, pyridine-, and pyridinium-assisted H^+ mobility in $HSiW_9V_3O_{40}^{6-}$, results which comprise the first homogeneous model for H^+ mobility on a heterogeneous metal oxide surface and, when combined with the study of reduced heteropolyanions ("heteropoly blues"),[17] a homogeneous model for H· ($H^+ + e^-$) spillover.

(7) The four-bond vanadium to tungsten coupling, $^4J_{V_3\text{-}O\text{-}W_{12}} = 4.0 \pm 0.5$ Hz, in $HSiW_9V_3O_{40}^{6-}$, a result that issues a warning against the use of only two-bond vanadium–tungsten and tungsten–tungsten couplings in making structural assignments.

The preparation of organic medium soluble vanadotungstates, the detailed studies of their protonation, deprotonation, and H^+ mobility, and the effects these have on their ^{29}Si, ^{31}P, and ^{183}W NMR are probably the most novel aspects of the present work. These studies establish $(Bu_4N)_{7-x}H_xSiW_9V_3O_{40}$ and $(Bu_4N)_{9-x}H_xP_2W_{15}V_3O_{62}$ as, perhaps, the polyoxoanions with surface charge density most thoroughly characterized in nonaqueous solvents. The establishment of polyoxoanion solution structures and diagnostic spectral features are a required foundation for subsequent catalytic and especially for mechanistic studies of polyoxoanions. For this reason, one focus of our work has been the determination of polyoxoanion compositions and structures in solution without a heavy dependence upon X-ray crystallography (although we have many cases where an accurate, single-crystal structure determination would be of considerable interest and collaborative efforts to obtain such structures are in progress). Repeated attempts to obtain diffraction data for well-formed crystals of $(Bu_4N)_4H_3SiW_9V_3O_{40}$ have failed, however, all crystals examined showing weak diffraction due, perhaps, to disorder problems.

Subsequent publications will report the preparation and characterization of the first vanadotungstate-supported organometallic compounds[1c] $CpTi\cdot SiW_9V_3O_{40}^{4-}$ and $CpTi\cdot P_2W_{15}V_3O_{62}^{6-}$, efforts to develop the catalytic chemistry of these and related species,[33] electrochemical studies of $H_xSiW_9V_3O_{40}^{x-7}$, $H_xP_2W_{15}V_3O_{62}^{x-9}$, and other vanadotungstates,[33] the preparation and support properties of $(Bu_4N)_9P_2W_{15}Nb_3O_{62}$,[34] catalytic studies of tungstate-supported Rh and Ir complexes,[35] catalytic epoxidation studies with a $Si_2W_{18}Nb_6O_{77}^{8-}$ catalyst precursor,[1a,36] FABMS of polyoxoanions of molecular weight 4000–8000 daltons,[9b] and our now complete studies of the disubstituted dimers $[PW_9M_2(H_2O)O_{34}]_2^{10-}$ and $[P_2W_{15}M_2(H_2O)O_{56}]_2^{12-}$.[1e,f,37]

(31) The question of the presence of H_3O^+ or H_2O could not be unambiguously answered for a sample of $(Bu_4N)_5H_4P_2W_{15}V_3O_{62}\cdot XH_2O$ [dried at 50 °C for 3 weeks (see Experimental Section)]. Due to its lower solubility, control experiments using 0.25 equiv of $(H_3O)_4SiW_{12}O_{40}$ indicated that up to 1 equiv of H_3O^+ (1715 cm^{-1}) could not be detected by conventional IR spectroscopy, although chemical evidence ($Bu_4N^+OH^-$ ^{31}P and ^{51}V NMR titration) is consistent with the absence of H_3O^+. A 1635-cm^{-1} band characteristic of H_2O was observed in the IR and the addition of a known amount of water followed by IR examination suggests that ca. 1 equiv of water is in fact present. [Efforts to confirm the presence of H_2O by thermal gravimetric analysis failed due to a gradually sloping base line and the uncertainty (±0.3%) in the final weight percent.]

(32) (a) "$Na_{12}P_2W_{15}O_{56}$" is a noncrystalline material that was previously formulated[32b] as "$Na_{12}P_2W_{16}O_{59}$" but is now thought to be largely, but perhaps not completely, $Na_{12}P_2W_{15}O_{56}\cdot XH_2O$.[32b] It is another example supporting our assertion[7a,b] that the combined use of oxygen analysis and FABMS can be a major step toward avoiding misformulated polyoxoanions in favorable cases. (b) See the references, discussion, and ref 3 in ref 1f.

(33) Finke, R. G.; Rapko, B., unpublished results.

(34) Finke, R. G.; Edlund, D.; Saxton, R. J. Jr., manuscript in preparation.

(35) Finke, R. G.; Edlund, D., unpublished results.

(36) Finke, R. G.; Droege, M. W., unpublished results.

(37) Finke, R. G.; Droege, M. W.; Domaille, P., manuscript in preparation.

Experimental Section

Materials. All compounds used were of reagent grade and were used as received except as otherwise indicated: $Na_2WO_4 \cdot 2H_2O$ (Spectrum); 3-Å Davidson molecular sieves, 1-methyl-2-pyrrolidinone, $NaVO_3$ (Fischer); 0.1 N $Bu_4N^+OH^-$/isopropyl alcohol; $Bu_4N^+Br^-$ (>98%) (Fluka); D_2O (Norell); Me_2SO-d_6 (Mallinckrodt); KCl, $Na_2SiO_3 \cdot 9H_2O$, DMF, Me_2SO, CH_3CN, CH_2Cl_2, MeOH, silicotungstic acid (Baker Analyzed); CD_3CN (Cambridge Isotope Laboratories); Amberlyst 15 ion-exchange resin, $Me_4N^+Cl^-$, pyridine, pyrrolidine, $Pr_4N^+Br^-$, $LiClO_4$, CaH_2, $Bu_4N^+OH^-$ (1 M in methanol), $Bu_4N^+OH^-$ (40% in water) (Aldrich). Dry acetonitrile was prepared by distillation from CaH_2 under nitrogen (after refluxing overnight) followed by standing for at least 48 h over ca. 30% by volume 3-Å molecular sieves previously activated under vacuum at 170 °C. Dry Me_2SO-d_6 was prepared by storage over activated 3-Å molecular sieves until no water could be observed by ^1H NMR. The Amberlyst resin was initially prepared by washing with neutral water followed by 2 N NaOH until the filtrate was clear, rewashing with water until the filtrate was neutral, then packing into a column and passing 0.1 N HCl through until the eluant tested acidic with pH paper, and then rewashing with neutral water until the eluant tested neutral. Colorless tetrabutylammonium hydroxide was standardized by titration with a standardized HCl solution, requiring the observation of identical end points when phenolphthalein and methyl red were used as indicators.

The α-$Na_{12}P_2W_{15}O_{56} \cdot 18H_2O$ preparation used was that listed originally as "$Na_{12}P_2W_{16}O_{59}$"[32] prepared by base degradation of α-$P_2W_{18}O_{62}^{6-}$.

Instrumentation/Analytical Procedures. UV-visible spectra were recorded by using a Cary 15 UV-vis spectrometer. IR spectra were recorded on a Sargent-Welch SP3-200 or a Beckman 4240 spectrometer. IR samples were prepared either as KBr disks or as CH_3CN solutions using either 0.1-mm path length CaF_2 (1800–1600 cm^{-1}) or 0.1-mm path length NaCl cells with CH_3CN in the reference cell. Spectra were calibrated by reference to the 1601-cm^{-1} band of polystyrene.

Early elemental analyses were obtained from Galbraith Laboratories, Inc., Knoxville, TN, and more recent analyses from E + R Microanalytical Laboratory, Inc., Corona, NY, and Mikroanalytisches Labor Pascher, Bonn, West Germany. The source of the analytical data is indicated with each analysis.

^{183}W, ^{31}P, ^{51}V, and ^{29}Si NMR spectra were recorded on a Nicolet NT 360 NMR system with field/frequency lock on appropriated deuterated solvents at 21 °C unless otherwise noted. Chemical shifts are reported in parts per million with negative values upfield of the standard.

^{183}W NMR spectra (15.04 MHz) were obtained using 10-mm-o.d., sample tubes and are referenced to saturated Na_2WO_4 in D_2O using the substitution method. Spectral parameters include pulse width = 70 μs (90° flip angle), acquisition time = 819.4 ms (1.22 Hz/data point), repetition rate = 819.6 ms, and sweep width = ±2500 Hz. An exponential line broadening of 1 Hz was used unless otherwise noted. The broad-band power amplifier was attenuated by 6 dB to prevent probe arcing. Acoustic probe ringing required the introduction of a 1000-μs delay before acquisition.

^{29}Si NMR spectra (71.74 MHz) were obtained using 12-mm-o.d. sample tubes and are referenced to Me_4Si in acetone-d_6 using the substitution method. Spectral parameters include pulse width = 20 μs (90° flip angle), acquisition time = 1.03 s (1.1 Hz/data point), repetition rate = 1.28 s, and sweep width = ±4000 Hz. An exponential line broadening of 1 Hz was used unless otherwise noted.

^{31}P NMR spectra (146.18 MHz) were obtained using 12-mm-o.d. tubes and are referenced to 1% phosphoric acid in D_2O by using the substitution method. Spectral parameters include pulse width = 20 μs (60° flip angle), acquisition time = 1.02 s (0.92 Hz/data point), repetition rate = 2.02 s, and sweep width = ±2000 Hz. An exponential line broadening of 0.1 Hz was employed.

^{51}V NMR spectra (94.92 MHz) were obtained using 12-mm-o.d. sample tubes and referenced to neat $VOCl_3$ by using the substitution method. Typical spectral parameters include pulse width = 20 μs (90° flip angle), acquisition time = 13.34 ms, repetition rate = 13.61 ms, and sweep width = ±19 000 Hz. An exponential line broadening of 25 Hz was employed unless otherwise noted. A preamp attenuation of 10–30 dB was applied as necessary to prevent receiver saturation. For all the above nuclei, line widths were obtained by best fitting to Lorentzian line shapes using standard Nicolet software and are corrected for exponential line broadening.

^1H NMR were recorded on a Varian XL-100 NMR spectrometer operating in the continuous-wave mode. Samples were reported using the δ scale and referenced to the residual ^1H impurity of the deuterated solvent relative to Me_4Si.

The operating parameters used at Du Pont to obtain the ^{51}V-decoupled ^{183}W NMR and 2-D INADEQUATE ^{183}W NMR have been reported previously.[18]

Potentiometric titrations were done by using a Corning calomel combination pH electrode attached to a Corning Model 125 pH meter operating with the millivolt scale. The system was calibrated by using commercially available solutions of pH 3, 7, and 10 prior to each use.

Solution molecular weights were determined by using a Beckman Instruments Spinco Model E Ultracentrifuge equipped with a scanning photoelectric system using the sedimentation equilibrium method.[38] Heteropolytungstate solutions were prepared by dissolving the sample in water, for tetramethylammonium salts, or acetonitrile, for tetrabutylammonium salts, containing an 0.1 M solution of the appropriate electrolyte ($Me_4N^+Cl^-$ or Bu_4N^+ PF_6^-) and diluting with this electrolyte solution until an absorbance of 0.2–0.4 (l = 1 cm) was observed at 250 nm. Using doubly sectored cells, concentration vs. distance data were obtained directly from the photoelectron scanner output. The rotation speed was 20 000 rpm and equilibrium was generally obtained after 16 h. The temperature was not regulated but measured at the end of each run. The concentration vs. distance data were evaluated as follows:

$$MW = \frac{2RT}{(1 - \bar{\nu}\rho)\omega^2} \frac{d \ln C}{dr^2}$$

where $R = 8.314 \times 10^7$ J K^{-1} mol^{-1}, $\bar{\nu}$ = partial specific volume, ρ = density of solution, $\omega = 2\pi/60$ (rpm), and $(d \ln C)/dr^2$ = slope obtained from a plot of ln (concentration) vs. (distance from the center of rotation)^2 as determined from the scanner output.

The solution density for measurements in water is 1.0 g/mL. The solution density for measurements in acetonitrile is 0.78 g/mL at the normal operating temperature. The partial specific volume was approximated by the apparent specific volume which was obtained by the method of densities using a calibrated 25-mL pycnometer.

Thermal gravimetric analyses were obtained by using a Du Pont Instruments 951 Thermogravimetric Analyzer with a 1090 thermal analyzer for data processing. Samples were run under air from 20 to 650 °C at a rate of 20 °C/min in early parts of this work and, more recently and preferably, at ≤12 °C. They were performed courtesy of Catalytica Associates, Mountain View, CA 94043. Both our recent TGA data and the literature[12d] indicate that results agreeing with calculated values to ≤±0.5 wt % can be generally obtained if slower heating rates (5 to ≤12 °C/min) are employed.

Fast atom bombardment mass spectra were obtained as previously described on a VG analytical ZAB-HF ultrahigh-resolution 8-kV mass spectrometer with a 11250 data system at the University of Illinois at Urbana with the assistance of Dr. J. C. Cook and Professor K. S. Suslick.

Preparation of A-β-$Na_9HSiW_9O_{34} \cdot 23H_2O$. This heteropolytungstate was prepared by a modified literature procedure.[10] $Na_2SiO_3 \cdot 9H_2O$, 60 g (0.21 mol), was dissolved in 400 mL of distilled water. $Na_2WO_4 \cdot 2H_2O$, 362 g (1.1 mol), was added and the solution stirred until homogeneous. HCl, 6 M, 200 mL (1.2 mol), was added slowly to the vigorously stirred solution. The gelatinous precipitate which forms during this acid addition was removed by filtration and the clear filtrate kept at 5 °C for several days. Filtration followed by air drying results in varying yields (50–80 g, 14–23%) of the white, crystalline solid.

Synthesis of $K_6HSiW_9V_3O_{40} \cdot 3H_2O$. In a typical preparation, 6.4 g (52 mmol) of sodium metavanadate was dissolved in 900 mL of hot water and cooled to room temperature. To this colorless, homogeneous solution, 8.4 mL (101 mmol) of 12 M HCl was added, resulting in a pale yellow, homogeneous solution (pH about 1.5). This was followed by addition of 48 g (16.9 mmol) of solid A-β-$Na_9HSiW_9O_{34} \cdot 23H_2O$ to the vigorously stirred solution. This solution rapidly develops a deep, cherry-red color as the $SiW_9O_{34}^{10-}$ dissolves. The resulting homogeneous solution was reacidified with 2.8 mL (33.6 mmol) of 12 M HCl, bringing the total H^+ added to 134.6 mmol (8.0 equiv). Next, 60 g (800 mmol) of solid KCl was added and the solution stirred until homogeneous. Methanol was then added until the total volume was approximately 2 L. The resulting precipitate was separated by filtration and recrystallized overnight from a hot, saturated pH 1.5 water/methanol solution. Filtration followed by air drying at 60 °C yields 37 g (82% yield). Anal.: H_2O (following drying at 25 °C under vacuum), calcd for $3H_2O$ 2.0%, found (by TGA weight loss up to 523 K) 1.7; K^+, calcd for $K_6HSiW_9V_3O_{40} \cdot 3H_2O$ 8.48%, found (E + R) 8.68%; Na^+, calcd 0.0, found <0.04%. IR (KBr disk): 1005 (w), 955 (m), 900 (s), 780 cm^{-1} (s, br). ^{183}W NMR (as Li^+ salt following metathesis with excess $LiClO_4$ ~ 1 g/mL D_2O): −110.4 (6 W), −112.9 ppm (3 W). ^{51}V NMR (~1 g/4 mL of D_2O; pD 2.3):[28a] −570 ppm ($\Delta\nu_{1/2}$ = 372 ± 6 Hz). For comparison, Pope et al.[5a] find that the α isomer A-α-$SiW_9V_3O_{40}^{7-}$ shows a ^{51}V NMR resonance at −566 ppm ($\Delta\nu_{1/2}$ = 130 Hz at 80 °C, pH 2).

(38) (a) Chervenka, C. H. "A Manual of Methods for the Analytical Ultracentrifudge"; Spinco Division of Beckman Instruments: Palo Alto, CA, 1969. (b) Fujita, H. "Foundations of Ultracentrifugal Analysis"; Wiley: New York, 1975; pp 308–313.

Forty grams of this compound was dissolved in water and passed down a column containing 50 g of Amberlyst 15 strongly acidic ion-exchange resin (4.7 mequiv/g) charged in the H^+ form. The colored solution was collected and the solvent removed under vacuum leaving 39 g of the free acid as an orange powder. ^{183}W NMR (~2 g/mL of D_2O; pD about 0.9):[28a] −120.0 (6 W, $\Delta\nu_{1/2}$ = 2.56 ± 0.09 Hz), −115.4 ppm (3 W, $\Delta\nu_{1/2}$ = 1.32 ± 0.07 Hz; $^2J_{W\text{-}O\text{-}W}$ = 16.4 ± 1.2 Hz. ^{29}Si NMR: 2 g/mL at −83.5 pm; $\Delta\nu_{1/2}$ = 1.48 ± 0.07 Hz; S/N = 177:1. ^{51}V NMR: −575 ppm; $\Delta\nu_{1/2}$ = 890 ± 8 Hz.

Preparation of $(Bu_4N)_4H_3SiW_9V_3O_{40}$. In a typical preparation, 40 g (14 mmol) of $K_6HSiW_9V_3O_{40}$ was dissolved in about 200 mL of pH 1.5 water and was added slowly to a stirring solution containing 20 g (62 mmol) of $Bu_4N^+Br^-$ in 100 mL of pH 1.5 water. After addition of the colored $SiW_9V_3O_{40}^{7-}$ solution was complete, the mixture was reacidified to pH 1.5 with 12 M HCl. The resulting precipitate was collected by filtration (note the filtrate is colorless at this point), washed with an equal volume of pH 1.5 water, and dried at 50 °C. The solid was then placed in a 150-mL beaker and dissolved in a minimum (about 50 mL) of warm acetonitrile, and the beaker was immersed in a capped jar containing dichloromethane. Following several days of vapor diffusion, red crystals of $(Bu_4N)_4H_3SiW_9V_3O_{40}$ appear. The yield is 29.5–36 g (58–70% based on $K_6HSiW_9V_3O_{40}\cdot 3H_2O$). Elemental analysis (Pascher) following overnight drying at 80 °C under vacuum: calcd (found) C, 22.28 (22.11); H, 4.27 (4.38); N, 1.62 (1.67); Si, 0.81 (0.79); W, 48.0 (47.7); V, 4.43 (4.28); O, 18.6 (17.9); Na, 0 (<0.01); K, 0 (<0.01); H_2O (by TGA loss up to 473 K) O (0); total, 100% (98.8%). The UV spectrum in CH_3CN exhibits end absorption with a shoulder at 250–260 nm, $\epsilon_{250} = 2.9 \times 10^4$, $\epsilon_{260} = 2.7 \times 10^4$ cm^{-1} mol^{-1} L. The visible spectrum also exhibits end absorption with a shoulder at approximately 500 nm, $\epsilon \sim 1020$ cm^{-1} mol^{-1} L. IR spectrum (CH_3CN solution): 1005 (w), 960 (m), 895 (s), 810 cm^{-1} (s). Solution molecular weight (in CH_3CN): calcd for $(Bu_4N)_2H_3SiW_9V_3O_{40}^{2-}$, 2963; found, 3096. ^{29}Si NMR in wet (10 equiv of water) CD_3CN shows only one line at −83.0 ppm (S/N = 112; $\Delta\nu_{1/2}$ = 0.52 ± 0.04 Hz). ^{51}V NMR in wet (10 equiv of water) CD_3CN shows only one line at −579 ppm (S/N = 82; $\Delta\nu_{1/2}$ = 1358 ± 4 Hz). ^{183}W NMR in wet (10 equiv of water) CD_3CN shows two lines at −108.4 (6 W, $\Delta\nu_{1/2}$ = 4.4 ± 0.2 Hz; S/N = 50) and at −110.1 ppm (3 W, $\Delta\nu_{1/2}$ = 4.0 ± 0.4 Hz; S/N = 25).

$(Bu_4N)_4H_3SiW_9V_3O_{40}$ is reasonably soluble (up to about 0.1 M) in such polar aprotic solvents as CH_3CN, Me_2SO, and DMF. It is somewhat soluble in nitromethane, methanol, and propylene carbonate and only slightly soluble to insoluble in water, alcohols, ethers, chlorinated hydrocarbons, aliphatic hydrocarbons, and aromatic hydrocarbons.

Potentiometric titrations for $(Bu_4N)_4H_3SiW_9V_3O_{40}$ were performed in CH_3CN, dry CH_3CN, Me_2SO, and DMF by using 1 M $Bu_4N^+OH^-$/methanol as the titrant. Other systems, such as in CH_3CN, using 40% $Bu_4N^+OH^-$/water or in dry acetonitrile using 0.1 N $Bu_4N^+OH^-$/isopropyl alcohol were also examined. Generally, the titrations were performed under a nitrogen atmosphere, to exclude CO_2, although for a given system such as 40% $Bu_4N^+OH^-$/water with CH_3CN solvent, identical results were observed in air.

In a typical experiment, the titration of $(Bu_4N)_4H_3SiW_9V_3O_{40}$ in CH_3CN using 1 M $Bu_4N^+OH^-$/methanol was performed as follows. Under nitrogen, 0.9500 g of $(Bu_4N)_4H_3SiW_9V_3O_{40}$ was dissolved in 30 mL of acetonitrile, and the potential of this stirring solution was recorded. Successive amounts of 1.0 M $Bu_4N^+OH^-$/MeOH were introduced in 0.2-equiv (28 μL) increments while the solution's potential was continuously monitored. The system was assumed to have reached equilibrium when no change in the solution's potential was observed over an approximately 30-s interval.

For all the systems described above, sharp breakpoints at 1 and 2 equiv of OH^- were observed. The addition of up to 40 total equiv of base resulted in no further potential increase and even a slight drop to more positive potential. Controls, where the solution's potential was monitored following addition of $Bu_4N^+OH^-$ to just the solvent, indicate the electrode's limiting response occurs near the potential which follows the second breakpoint (Figure 2, supplementary material).

The IR of $(Bu_4N)_4H_3SiW_9V_3O_{40}$ in the 1800–1600-cm^{-1} region was obtained to attempt to identify the presence of either H_3O^+ or lattice water. Both the H_3O^+ source, $(H_3O)_4SiW_{12}O_{40}$, and $(Bu_4N)_4H_3SiW_9V_3O_{40}$ were dried at 80 °C under vacuum before use. Dry CH_3CN was used to prepare a concentrated (1 g of sample/5-mL total volume) solution of $(Bu_4N)_4H_3SiW_9V_3O_{40}$. An initial IR examination of the solvent itself confirmed the absence of water. While examining the spectra in both the absorbance and transmittance modes, successive equivalents of water were added to the $(Bu_4N)_4H_3SiW_9V_3O_{40}$ to obtain control spectra where known amounts of H_2O were present. As a control experiment for detecting the presence of H_3O^+, an IR spectrum of $(H_3O)_4SiW_{12}O_{40}$ in dry CH_3CN at one-fourth the concentration of the $(Bu_4N)_4H_3SiW_9V_3O_{40}/CH_3CN$ solution examined above was obtained. The conclusion from these controls is that at least 1 equiv of either H_3O^+ or H_2O could be detected by IR under the experimental conditions.

Preparation of $(Bu_4N)_5H_2SiW_9V_3O_{40}$. $(Bu_4N)_4H_3SiW_9V_3O_{40}$, 2 g (0.58 mmol), was dissolved in 20 mL of acetonitrile. $Bu_4N^+OH^-$/MeOH, 1.0 M, 580 μL (1 equiv), was introduced to this stirring solution by syringe, and the resulting solution was stirred for 5 min. All solvent was removed at room temperature under high vacuum to yield a red powder. ^{183}W NMR (2 g/3 mL of dry CD_3CN) yields no discernable resonances; following the addition of 100 equiv of water, two resonances at −109.5 (3 W) and −105.0 ppm (6W) were observed. ^{29}Si NMR (2 g/3 mL of CD_3CN) show a singlet at −84.19 ppm ($\Delta\nu_{1/2}$ = 3.8 ± 0.3 Hz). Following the addition of 100 equiv of water a singlet at −83.85 ppm ($\Delta\nu_{1/2}$ = 1.06 ± 0.04 Hz) is observed. ^{51}V NMR (2 g/3 mL of CD_3CN) shows three resonances at −554 ($\Delta\nu_{1/2} \sim 256 \pm 7$ Hz), −562 ($\Delta\nu_{1/2} \sim 498 \pm 9$ Hz), and −580 ppm ($\Delta\nu_{1/2} \sim 2257 \pm 18$ Hz). Due to overlapping resonances, integrations were not attempted. Following the addition of 100 equiv of water a singlet at −575 ppm ($\Delta\nu_{1/2} \sim 2343 \pm 18$ Hz) is observed. The IR spectrum is provided in Figure 3, supplementary material.

Preparation of $(Bu_4N)_6HSiW_9V_3O_{40}$. $(Bu_4N)_4H_3SiW_9V_3O_{40}$, 2 g (0.58 mmol), was dissolved in 20 mL of acetonitrile. $Bu_4N^+OH^-$/MeOH, 1.0 M, 1.16 mL (2 equiv), was introduced to the stirring solution by syringe and the resulting solution stirred for 5 min. All solvent was removed at room temperature under high vacuum to yield a red solid. ^{29}Si NMR (1 g/2 mL of CD_3CN) shows one line at −84.19 kppm ($\Delta\nu_{1/2}$ = 1.03 ± 0.03 Hz). ^{51}V NMR (1 g/3 mL of CD_3CN) shows two lines at −545 ($\Delta\nu_{1/2}$ = 106 ± 1 Hz) and −576 ppm ($\Delta\nu_{1/2}$ = 1871 ± 25 ppm). ^{183}W NMR (1 g/mL of CD_3CN) shows five lines at −83.3 (1 W, $\Delta\nu_{1/2}$ = 9.4 ± 0.3 Hz), −88.1 (2 W, $\Delta\nu_{1/2}$ = 4.23 ± 0.05 Hz), −93.3 (2 W, ($\Delta\nu_{1/2}$ = 3.24 ± 0.06 Hz), −99.4 (2 W, about 80-Hz wide), and −112.9 ppm (2 W, ($\Delta\nu_{1/2}$ = 2.64 ± 0.08 Hz). The IR spectrum for this compound is included in Figure 3, supplementary material.

Preparation of $(Bu_4N)_7SiW_9V_3O_{40}$. $(Bu_4N)_4H_3SiW_9O_{40}$, 2 g (0.58 mmol), was dissolved in 20 mL of acetonitrile. $Bu_4N^+OH^-$/MeOH, 1.0 M, 1.74 mL (3 equiv), was introduced to this stirring solution by syringe and the resulting solution stirred for 5 min. All solvent was then removed at room temperature under high vacuum to yield a red powder. ^{183}W (1 g/mL of CD_3CN): −81.1 (6 W, $^2J_{W\text{-}O\text{-}W}$ = 13.4 ± 1.2 Hz), −101.4 ppm (3 W, $^2J_{W\text{-}O\text{-}W}$ = 13.4 ± 1.2 Hz). ^{51}V NMR (1 g/3 mL of CD_3CN) shows one major line at −531 ppm ($\Delta\nu_{1/2}$ = 954 ± 9 Hz). ^{29}Si NMR (1 g/mL of CD_3CN) shows one line at −83.38 ppm ($\Delta\nu_{1/2}$ = 1.13 ± 0.04 Hz). All spectra also show the presence of some $(Bu_4N)_6HSiW_9V_3O_{40}$. The IR spectrum for this compound is included in Figure 3, supplementary material.

Reaction of $(Bu_4N)_4H_3SiW_9V_3O_{40}$ with 4 Equiv of $Bu_4N^+OH^-$. $(Bu_4N)_4H_3SiW_9V_3O_{40}$, 2 g (0.58 mmol), was dissolved in 20 mL of acetonitrile. $Bu_4N^+OH^-$/MeOH, 1.0 M, 2.34 mL (4 equiv), was introduced to this stirring solution by syringe and the resulting solution stirred for 5 min. All solvent was then removed at room temperature under high vacuum, yielding a red powder. ^{183}W NMR, ^{51}V NMR, and ^{29}Si NMR are essentially identical with those observed for $(Bu_4N)_4H_3SiW_9V_3O_{40}$ + 3 equiv of $Bu_4N^+OH^-$ only now the resonances assigned to $(Bu_4N)_6HSiW_9V_3O_{40}$ have disappeared. Integration of all other resonances in the ^{51}V NMR yields 23% of the intensity of the main signal at about −530 ppm assigned to $(Bu_4N)_7SiW_9V_3O_{40}$. Similarly, integration of all other resonances in the ^{29}Si NMR spectrum yields 29% of the intensity of the resonance of −83.4 ppm, assigned to $(Bu_4N)_7SiW_9V_3O_{40}$.

Preparation of $K_8HP_2W_{15}V_3O_{62}\cdot 9H_2O$. Sodium metavanadate, 4 g (32.8 mmol), was dissolved in 700 mL of hot water and cooled to room temperature followed by the addition of 16 mL of 6 M HCl (96 mmol). To this pale yellow, rapidly stirred solution, 46 g (10.7 mmol) of solid $Na_{12}P_2W_{15}O_{56}\cdot 18H_2O$ was added slowly. The solution becomes homogeneous within a few minutes becoming red-orange in color. Stirring was continued for an additional 10 min after the solution becomes homogeneous followed by addition of 100 g (1350 mmol) of solid KCl. The resulting precipitate was isolated by filtration and crystallized from hot pH 1.5 water overnight (the total solution volume for this crystallization being about 75 mL). The precipitate was isolated by filtration and dried in air in 60 °C to yield 38 g (80%) of a crystalline orange solid. ^{31}P NMR in pD 1.9 D_2O shows two lines at −6.7 and −14.3 ppm. Analysis for $K_8HP_2W_{15}V_3O_{62}\cdot 9H_2O$: K^+ calcd 7.31%, found (Galbraith) 7.34%; Na^+ calcd 0.0%, found (E + R) <0.04%. H_2O (by TGA weight loss at 200 °C) calcd for $9H_2O$, 3.71%; found, 3.68%. ^{51}V NMR (prepared by ion exchange to the Li^+ salt) shows a single resonance at −504 ppm ($\Delta\nu_{1/2}$ = 110 Hz) at 30 °C, pD 6.3. ^{183}W NMR (prepared by ion exchange to the Li^+ salt, undecoupled at 30 °C, pD 6.3): −158.2 (3 W), −178.7 (6 W, $\Delta\nu_{1/2}$ = 54 Hz), and −226.7 (6 W) (Figure 15B). Thirty eight grams of the potassium salt was dissolved in about 200 mL of water and was passed down 50 g of the Amberlyst 15 strongly acidic cation exchange resin charged in the H^+. No retention of the colored material is noted

and the colored eluant was collected and the water removed by rotary evaporation of the solvent under water aspirator vacuum using a steam bath. About 32 g of the orange solid was recovered. ^{31}P NMR (2 g/mL of D_2O; pD about 1) shows two lines at −7.6 and −14.3 ppm. ^{51}V NMR (0.5 g/3 mL of D_2O, 21 °C) shows the major resonance at −576 ppm ($\Delta\nu_{1/2}$ = 468 ± 9 Hz) and a smaller (<5%) resonance at −558 ppm. IR (KBr pellet): 1075 (s), 1045 (m), 1010 (sh), 935 (m), 875 (w), 765 cm^{-1} (s, br).

Preparation of $TMA_6H_3P_2W_{15}V_3O_{62}\cdot 6H_2O$. Sodium metavanadate, 0.95 g (7.8 mmol), was dissolved in 175 mL of water and cooled to room temperature and 4 mL of 6 M (24 mmol) HCl added. To the pale yellow, rapidly stirred solution, 11 g (2.55 mmol) of solid α-$Na_{12}P_2W_{15}O_{56}\cdot 18H_2O$ was added slowly. Stirring was continued for 10 min after the solution becomes homogeneous and the 8 g (73 mmol) of solid $Me_4N^+Cl^-$ was added. The resulting precipitate was isolated by filtration and crystallized from hot, saturated (about 400-mL total volume) pH 1.5 water, yielding about 9 g (78% yield) of crystalline orange solid. Elemental analysis (Pascher) calcd (found) for $(Me_4N)_6H_3P_2W_{15}V_3O_{62}\cdot 6H_2O$: C, 6.37 (6.41); H, 1.92 (1.84); N, 1.86 (1.90); V, 3.38 (3.30); W, 61.0 (61.0); P, 1.37 (1.38); Na^+ (E + R) calcd 0, found <0.04%. H_2O, (for product dried at 40 °C under vacuum for 5 h) as determined by TGA weight loss below 200 °C, 2.40 (2.49). ^{31}P NMR (following ion exchange to the Li^+ salt) shows two lines at −6.9 and −14.0 ppm. Solution molecular weight for $P_2W_{15}V_3O_{62}^{9-}$ (in 0.1 M $Me_4N^+Cl^-$/water): calcd 3964, found 3622 (Figure 1B, supplementary material). ^{51}V NMR (following ion exchange to the Li^+ salt) shows one line at −504 ppm, $\Delta\nu_{1/2}$ = 110 Hz, 30 °C, pD 6.3.

Preparation of $(Bu_4N)_5H_4P_2W_{15}V_3O_{62}$. $K_8HP_2W_{15}V_3O_{62}\cdot 9H_2O$, 35 g (7.6 mmol), was dissolved in 200 mL of pH 1.5 water and added dropwise to a stirring solution containing 25 g (78 mmol) of $Bu_4N^+Br^-$ in 200 mL of pH 1.5 water, the pH of the $Bu_4N^+Br^-$ solution being continuously monitored with a pH meter and 6 M HCl added as necessary to keep the observed pH range between 1.4 and 1.6. After the addition of the orange $K_8HP_2V_3O_{62}$ solution to the $Bu_4N^+Br^-$ solution was completed, the resulting precipitate was filtered and washed with 200 mL of pH 1.5 water. The sample then was dissolved in 200 mL of warm DMF and passed through a column containing 100 mL (1.8 mequiv/mL) of Amberlyst 15 cation-exchange resin charged in the Bu_4N^+ form. The colored solution passes through the column without apparent retention, was collected, and the total volume was reduced to approximately 50 mL by rotary evaporation at reduced, water-aspirator pressure while being heated over a steam bath. This concentrated heteropolyanion solution was added dropwise to 1 L of vigorously stirred pH 1.5 water, the pH being maintained between 1.5 and 1.6 by addition of 6 M HCl as necessary. After the addition of the heteropolyanion solution was completed, the resulting suspension is stirred for an additional hour, filtered, and dried at 50 °C for 5 days yielding 42 g of orange powder (98% based on $K_8HP_2W_{15}V_3O_{62}$). ^{1}H NMR (CD_3CN) of this material shows the characteristic resonances for Bu_4N^+ and DMF [with no H_2O or H_3O^+ resonances observed (ca. 0.05 equiv detectable)]. Calculated ratio for 5 $(RCH_2)_4N^+$ vs. $(CH_3)_2NCHO$ is 0.150, found 0.13. Elemental analysis (E + R) calcd for $(Bu_4N)_5H_4P_2W_{15}V_3O_{62}\cdot$DMF: C, 18.92; H, 3.62; N, 1.60, K, 0. Calcd for $(Bu_4N)_5H_4P_2W_{15}V_3O_{62}\cdot H_2O\cdot$DMF: C, 18.90; H, 3.66; N, 1.59; K, 0. Found: C, 19.09; H, 3.75; N, 1.49; K, <0.05%.

Following additional heating at 50 °C, 1 atm for 3 weeks all DMF is removed as indicated by IR (<0.02 equiv detectable) and ^{1}H NMR. TGA calculated residue for $(Bu_4N)_5H_4P_2W_{15}V_3O_{62}$ (assuming P_2O_5 + $15WO_3$ + $^3/_2V_2O_5$) at 650 °C = 73.4; for $(Bu_4N)_5H_4P_2W_{15}V_3O_{62}\cdot H_2O$ at 650 °C = 73.2; found 73.1. An IR control using $(H_3O)_4SiW_{12}O_{40}$ indicates that 1 equiv of H_3O^+ would be at the limits of detection (0.5% transmittance). TGA shows a small, gradual 0.82% weight loss from 30 to 220 °C.

^{31}P NMR (0.032 M in 1:1 CH_3CN/CD_3CN at 21 °C) yields two lines at −7.4 ppm ($\Delta\nu_{1/2}$ = 12.1 ± 0.2 Hz) and −13.1 ppm ($\Delta\nu_{1/2}$ = 4.01 ± 0.08 Hz). ^{51}V NMR (0.032 M in 1:1 CH_3CN/CD_3CN at 21 °C) shows a single line at −585 ppm ($\Delta\nu_{1/2}$ = 2026 ± 13 Hz). ^{183}W NMR (0.032 M in 1:1 CH_3CN/CD_3CN at 21 °C) shows three lines at −118.8 (1 W, $\Delta\nu_{1/2}$ = 5.9 ± 0.3 Hz), −163.2 (2 W, $\Delta\nu_{1/2}$ = 5.8 ± 0.4 Hz), and −172.4 ppm (2 W, $\Delta\nu_{1/2}$ = 20.7 ± 1.0 Hz). Addition of 100 equiv of H_2O at 21 °C results in a sharpening of the ^{31}P NMR lines to −7.5 ($\Delta\nu_{1/2}$ = 3.99 ± 0.04 Hz) and −13.3 ppm ($\Delta\nu_{1/2}$ = 2.61 ± 0.05 Hz). ^{183}W NMR (0.032 M in 1:1 CH_3CN/CD_3CN at 21 °C) shows three lines at −121.5 ($\Delta\nu_{1/2}$ = 2.6 ± 0.2 Hz), −167.0 ($\Delta\nu_{1/2}$ = 2.6 ± 0.2 Hz), and −174.3 ppm ($\Delta\nu_{1/2}$ = 19.8 ± 0.7 Hz). ^{51}V NMR (0.032 M in 1:1 CD_3CN/CH_3CN at 21 °C) shows a single line at −589 ppm ($\Delta\nu_{1/2}$ = 1059 ± 12 Hz).

It should be emphasized that in one instance, this procedure led to a heteropolyanion of different composition. Following drying for several days at 50 °C the elemental analysis (E + R) indicates the following composition. Calcd for $(Bu_4N)_6H_3P_2W_{15}V_3O_{62}\cdot$4DMF: C, 22.21; H, 4.53; N, 2.91. Found: C, 22.69; H, 4.32; N, 2.45. ^{1}H NMR (Me_2SO-d_6): calculated ratio of $(CH_3)_2NCHO$ vs. $(RCH_2)_4N^+$, 0.67; found, 0.63.

This compound is generally soluble, although to a lesser extent, in the same solvents as its $(Bu_4N)_4H_3SiW_9V_3O_{40}$ analogue, with solutions as concentrated as 0.1 M possible only in the most polar (DMF, Me_2SO) solvents. This compound is light-sensitive both in solution and in the solid state with the appearance of the green color indicative of the V(V) to V(IV) reduction of the heteropolyanion developing over several days, so that all samples of this compound were routinely protected from light. This compound appears to be extremely sensitive to alcohols, with the irreversible development of multiple species indicated by ^{31}P NMR immediately following exposure to methanol. Recrystallization from $DMF/CHCl_3$ using a vapor-diffusion technique can be accomplished but in our hands inevitably results in the development of varying (but always >5%) amounts of other species as indicated by ^{31}P NMR.

If the ion-exchange step is omitted, the trisubstituted heteropolyanion can be crystallized but as a mixed $(Bu_4N)^+$, K^+, acid salt in fair (69%) yield. ^{31}P NMR shows two lines at −7.5 and −13.2 ppm. ^{51}V NMR shows a single line at −582 ppm ($\Delta\nu_{1/2}$ = 1610 ± 9 Hz). ^{183}W NMR shows three lines at −120.4 (1 W), −160.8 (2 W), and −163.8 ppm (2 W), with the −160.8 ppm line being much more broad than the other two. Elemental analyses (Pascher) following drying at room temperature under high vacuum for several hours: calcd (found) for $(Bu_4N)_3KH_5P_2W_{15}V_3O_{62}\cdot$5DMF: C, 14.82 (14.65); H, 2.90 (3.00); N, 2.20 (2.06); P, 1.22 (1.16); W, 54.1 (52.9); V, 3.00 (2.88); O, 21.0 (18.8); K, 0.77 (0.70).

Preparation of $(Bu_4N)_6H_3P_2W_{15}O_{62}$. $(Bu_4N)_5H_4P_2W_{15}V_3O_{62}$, 0.5 g (0.097 mmol), was dissolved in 10 mL of CH_3CN. Freshly titrated $Bu_4N^+OH^-/H_2O$, 135 μL (1 equiv), was added by syringe, the solution stirred for 5 min, and the solvent completely removed at room temperature under high vacuum to yield an orange solid which was then pumped on for an additional ca. 0.5 h. ^{31}P NMR (0.032 M in 1:1 CH_3CN/CD_3CN at 21 °C) shows two lines at −7.2 ($\Delta\nu_{1/2}$ = 16.8 ± 0.3 Hz) and −13.6 ppm ($\Delta\nu_{1/2}$ = 5.5 ± 0.2 Hz). ^{51}V NMR (0.032 M in 1:1 CH_3CN/CD_3CN, 21 °C) shows a single line at −562 ppm ($\Delta\nu_{1/2}$ = 2080 ± 20 Hz).

Preparation of $(Bu_4N)_7H_2P_2W_{15}V_3O_{62}$. The procedure for the preparation of $(Bu_4N)_6H_3P_2W_{15}V_3O_{62}$ was repeated only here 270 μL (2 equiv) of $Bu_4N^+OH^-/H_2O$ was added. ^{31}P NMR (0.032 M 1:1 CH_3CN/CD_3CN, 21 °C) shows two lines at −7.2 ($\Delta\nu_{1/2}$ = 15.1 ± 0.2 Hz) and −13.9 ppm ($\Delta\nu_{1/2}$ = 4.00 ± 0.04 Hz). ^{51}V NMR (0.032 M in 1:1 CH_3CN/CD_3CN, 21 °C) shows a single line at −516 ppm ($\Delta\nu_{1/2}$ = 1350 ± 30 Hz).

Preparation of $(Bu_4N)_8HP_2W_{15}V_3O_{62}$. The procedure for the preparation of $(Bu_4N)_6H_3P_2W_{15}V_3O_{62}$ was repeated only here 3 equiv (405 μL) of $Bu_4N^+OH^-/H_2O$ was added. ^{31}P NMR (0.032 M in 1:1 CH_3CN/CD_3CN, 21 °C) shows two peaks at −7.0 ($\Delta\nu_{1/2}$ = 6.3 ± 0.1 Hz) and −14.2 ppm ($\Delta\nu_{1/2}$ = 2.23 ± 0.08 Hz). ^{51}V NMR (0.032 M in 1:1 CH_3CN/CD_3CN, 21 °C) shows a line at −489 ppm ($\Delta\nu_{1/2}$ = 562 ± 10 Hz).

Preparation of $(Bu_4N)_9P_2W_{15}V_3O_{62}$. The procedure for the preparation of $(Bu_4N)_6H_3P_2W_{15}V_3O_{62}$ was repeated only here 4 equiv (540 μL) of $Bu_4N^+OH^-/H_2O$ was added. ^{31}P NMR (0.032 M in 1:1 CH_3CN/CD_3CN, 21 °C) shows two peaks at −6.99 ($\Delta\nu_{1/2}$ = 1.76 ± 0.06 Hz) and −14.7 ppm ($\Delta\nu_{1/2}$ = 1.93 ± 0.05 Hz). ^{51}V NMR (0.032 M in 1:1 CH_3CN/CD_3CN, 21 °C) shows the single major line at −481 ppm ($\Delta\nu_{1/2}$ = 245 ± 3 Hz) and clearly a second resonance at −510 ppm with approximately 2% of the intensity of the −481 ppm resonance. ^{183}W NMR (0.032 M in 1:1 CH_3CN/CD_3CN, 21 °C) shows three lines at −139.5 (1 W, $\Delta\nu_{1/2}$ = 3.4 ± 0.4 Hz), −168.3 (2 W, $\Delta\nu_{1/2}$ (estimated due to low S/N at 72 Hz), and −211.8 ppm (2 W, $\Delta\nu_{1/2}$ = 3.0 ± 0.2 Hz).

Reaction of $(Bu_4N)_5H_4P_2W_{15}V_3O_{62}$ + 5$Bu_4N^+OH^-$. The procedure for the preparation of $(Bu_4N)_6H_3P_2W_{15}V_3O_{62}$ was repeated only here 675 μL of $Bu_4N^+OH^-/H_2O$ was added. The ^{31}P and ^{51}V NMR spectra appear identical with those observed following addition of 4 equiv of $Bu_4N^+OH^-$ to $(Bu_4N)_5H_4P_2W_{15}V_3O_{62}$; i.e., no decomposition was detectable due to the additional equivalents of OH^-.

Acknowledgment. Support from NSF Grant CHE-8313459 and from Dreyfus Teacher-Scholar (1982–1987) and Alfred P. Sloan (1982–1984) Fellowships to R.G.F. is gratefully acknowledged as is support from a Guggenheim Fellowship to R.G.F. (1984–1985) during which time this manuscript was prepared. We also appreciate the assistance of Dr. Jere Fellmann of Catalytica Associates, Inc., in obtaining the TGA results, of Dr. C. E. Klopfenstein for his assistance in obtaining NMR spectra (University of Oregon), and of Professor Michael Pope for helpful discussions in the early stages of these studies. FAB mass spectra were obtained in the mass spectroscopy facility of the School of Chemical Sciences, University of Illinois, supported in part by

NIH GM-27029 with the assistance of Dr. J. C. Cook and Professor K. S. Suslick; the ZAB mass spectrometer was purchased in part by grants from the Division of Research Resources, NIH (RR01575), and from the NSF (PCM-8121494).

Registry No. $K_6HSiW_9V_3O_{40}\cdot 3H_2O$, 101056-07-9; $K_4H_3SiW_9V_3O_4$, 91523-04-5; $H_7SiW_9V_3O_{40}$, 101056-06-8; $TBA_4H_3SiW_9V_3O_{40}$, 92816-61-0; $TBA_5H_2SiW_9V_3O_{40}$, 101033-41-4; $TBA_6HSiW_9V_3O_{40}$, 101033-39-0; $TBA_7SiW_9V_3O_{40}$, 101033-40-3; $K_8HP_2W_{15}V_3O_{62}\cdot 9H_2O$, 101165-00-8; $TMA_6H_3P_2W_{15}V_3O_{62}\cdot 6H_2O$, 101164-99-2; $TBA_5H_4P_2W_{15}V_3O_{62}$, 101164-94-7; $TBA_6H_3P_2W_{15}V_3O_{62}$, 101164-95-8; $TBA_7H_2P_2W_{15}V_3O_{62}$, 101164-96-9; $TBA_8HP_2W_{15}V_3O_{62}$, 101164-97-0; $TBA_9P_2W_{15}V_3O_{62}$, 101078-21-1; $Na_{12}P_2W_{15}O_{56}$, 84750-84-5; A-β-$Na_9HSiW_9O_{34}$, 91686-50-9; $Na_{12}P_2W_{16}O_{59}$, 65046-52-8; $Na_2SiO_3\cdot 9H_2O$, 13517-24-3; $Na_2WO_4\cdot 2H_2O$, 10213-10-2; $NaVO_3$, 13718-26-8; H^+, 12408-02-5; ^{29}Si, 14304-87-1; V, 7440-62-2; ^{183}W, 14265-81-7; pyridine, 110-86-1.

Supplementary Material Available: Four figures showing the following: Figure 1, plots of the ultracentrifugation molecular weight measurements for $(Bu_4N)_4H_3SiW_9V_3O_{40}$ in CH_3CN and $(Me_4N)_6H_3P_2W_{15}V_3O_{62}$; Figure 2, IR spectra while monitoring the deprotonation of $(Bu_4N)_4H_3SiW_9V_3O_{40}$ with $Bu_4N^+OH^-$/MeOH; Figure 3, sample potentiometric titration of $(Bu_4N)_4H_3SiW_9V_3O_{40}$ with $Bu_4N^+OH^-$/MeOH; and Figure 4, IR spectra while monitoring the deprotonation of $(Bu_4N)_6H_3P_2W_{15}V_3O_{62}$ with $Bu_4N^+OH^-/H_2O$ (5 pages). Ordering information is given on any current masthead page.

Evidence for a Rate-Determining Solvation Change in Methyl Transfer to Water. Solvent Dependence of H_2O/D_2O Kinetic Isotope Effects

Joseph L. Kurz,* Jasun Lee, Mark E. Love, and Susan Rhodes

Contribution from the Department of Chemistry, Washington University, St. Louis, Missouri 63130. *Received October 2, 1985*

Abstract: When H_2O is a dilute (<1 M) solute in CH_3CN or sulfolane, the rate of methyl transfer from CH_3X to H_2O is first order both in $[CH_3X]$ and in $[H_2O]$, but H_2O and D_2O react at the same rate ($k_H/k_D = 1.00 \pm 0.01$ for $X^- = OClO_3^-$ or thiophene). The analogous methyl transfers in CH_3CN at 25 °C from the same X^-'s to CH_3OH have $k_H/k_D = 1.07$ and 1.05 and to $(CH_3)_3COH$ have 1.12 and 1.07. In CH_3CN/H_2O (or ROH) solvent mixtures, as the H_2O (or ROH) content is increased to mole fractions >0.5, k_H/k_D for five of these six reactions increases sharply to the values observed in near H_2O or ROH: at 25 °C for $X^- = OClO_3^-$ and thiophene, respectively, $k_H/k_D = 1.20$ and 1.13 for H_2O, 1.22 and 1.15 for CH_3OH, and 1.08 and 1.12 for $(CH_3)_3COH$. Comparison of these k_H/k_D values to known values of deuterium fractionation factors for CH_3OH, H_3O^+, and $CH_3OH_2^+$ suggests the following: (a) for $CH_3X + H_2O$, there is little or no positive charge ($\delta = 0.00 \pm 0.04$) on the nucleophilic oxygen in the transition state. (b) For $CH_3X + CH_3OH$ or $(CH_3)_3COH$, that charge is larger than for H_2O. (c) The activation process in these methyl transfers (except for $CH_3OClO_3 + (CH_3)_3COH$) is predominantly a change in solvation of a preassociated H_2O (or ROH), CH_3X pair and, in the transition state, the solvation is more product-like than is the internal charge distribution. These inferences are consistent with a partly coupled mechanism for methyl transfer to H_2O.

Aliphatic nucleophilic substitutions in solution constitute one of the most exhaustively studied sets of organic reactions. However, several anomalous observations exist which imply that one of the most studied subsets of those reactions, nucleophilic attack by H_2O on methyl or primary alkyl groups (eq 1), does

$$H_2O + RCH_2X \rightarrow H_2O^+CH_2R + X^- \quad (1)$$

not take place via the generally accepted S_N2 mechanism or its ion pair variant. Those observations recently have been reviewed;[1] they suggest that the activation process is almost entirely a fluctuation in *solvent* configuration and does *not* involve significant H_2O–C bond formation or C–X bond cleavage.

The H_2O/D_2O kinetic isotope effect (KIE) on the rate of such a displacement by water provides a direct probe of the extent of H_2O–C bond formation during the activation process.[2] If this KIE is measured by changing the solvent from H_2O to D_2O, then the resulting k_{H_2O}/k_{D_2O} rate constant ratio is a product of two factors: the desired secondary deuterium KIE on the nucleophilicity of water and an isotopic *solvent effect* on the rate. The presence of that solvent effect renders uncertain any estimation of the extent of H_2O–C bonding present in the transition state which is based on the observed value of that k_{H_2O}/k_{D_2O} ratio. Prior to the work discussed here,[3] published values of k_{H_2O}/k_{D_2O} referred to such a combined change in solvent and in nucleophile.

The purpose of the work presented here was to reduce that uncertainty. Methyl transfers to H_2O and D_2O from three CH_3X compounds with two different charges were studied in two aprotic solvents: rate laws were determined and H_2O/D_2O KIE's were measured for reactions of 1-methylthiophenium ion ($MeTh^+$), methyl perchlorate ($MeOClO_3$), and methyl trifluoromethanesulfonate (MeOTf) with *dilute* solutions of water in acetonitrile (MeCN) and tetrahydrothiophene 1,1-dioxide ($TMSO_2$; tetramethylenesulfone or sulfolane), and alkyl substituent effects on the KIE's were explored via the reactions of ROL [R = CH_3 or $(CH_3)_3C$ (*t*-Bu); L = H or D] with $MeTh^+$ and $MeOClO_3$ and of L_2O with ethyl perchlorate ($EtOClO_3$). Also, the magnitudes of the isotopic *solvent* effects were measured by varying the solvent compositions over the full range from dilute solutions of the three nucleophiles (ROL or L_2O) in MeCN to pure ROL and L_2O. All of the observations are consistent with a mechanism in which the activation process is primarily a solvation change, and many of the observations are *not* consistent with the traditional S_N2

(1) Kurz, J. L.; Kurz, L. C. *Isr. J. Chem.*, in press.
(2) Schowen, R. L. *Prog. Phys. Org. Chem.* **1972**, *9*, 303-304.

(3) Preliminary reports of some of the observations discussed here were presented in ref 4 and 5. Small differences between rate constants and KIE's given here and in those references reflect the results of later measurements or of reanalysis of the original data; qualitative conclusions in those references remain unchanged.

0002-7863/86/1508-2960$01.50/0